the Takeda Scientific Foundation; and the Japan Vascular Disease Research Foundation.

Conflict of interest: none declared.

References

1. Adams RH, Alitalo K. Molecular regulation of angiogenesis and lymphangiogenesis. *Nat Rev Mol Cell Biol* 2007;**8**:464–478.
2. Alitalo K, Tammela T, Petrova TV. Lymphangiogenesis in development and human disease. *Nature* 2005;**438**:946–953.
3. Szuba A, Rockson SG. Lymphedema: anatomy, physiology and pathogenesis. *Vasc Med* 1997;**2**:321–326.
4. Mortimer PS. Therapy approaches for lymphedema. *Angiology* 1997;**48**: 87–91.
5. Kligman L, Wong RK, Johnston M, Laetsch NS. The treatment of lymphedema related to breast cancer: a systematic review and evidence summary. *Support Care Cancer* 2004;**12**:421–431.
6. Oh SJ, Jeltsch MM, Birkenhager R, McCarthy JE, Weich HA, Christ B *et al.* VEGF and VEGF-C: specific induction of angiogenesis and lymphangiogenesis in the differentiated avian chorioallantoic membrane. *Dev Biol* 1997; **188**:96–109.
7. Saito Y, Nakagami H, Morishita R, Takami Y, Kikuchi Y, Hayashi H *et al.* Transfection of human hepatocyte growth factor gene ameliorates secondary lymphedema via promotion of lymphangiogenesis. *Circulation* 2006;**114**:1177–1184.
8. Szuba A, Skobe M, Karkkainen MJ, Shin WS, Beynet DP, Rockson NB *et al.* Therapeutic lymphangiogenesis with human recombinant VEGF-C. *FASEB J* 2002;**16**:1985–1987.
9. Makinen T, Veikkola T, Mustjoki S, Karpanen T, Catimel B, Nice EC *et al.* Isolated lymphatic endothelial cells transduce growth, survival and migratory signals via the VEGF-C/D receptor VEGFR-3. *EMBO J* 2001;**20**:4762–4773.
10. Nuki C, Kawasaki H, Kitamura K, Takenaga M, Kangawa K, Eto T *et al.* Vasodilator effect of adrenomedullin and calcitonin gene-related peptide receptors in rat mesenteric vascular beds. *Biochem Biophys Res Commun* 1993;**196**:245–251.
11. Jougasaki M, Wei CM, Aarhus LL, Heublein DM, Sandberg SM, Burnett JC Jr. Renal localization and actions of adrenomedullin: a natriuretic peptide. *Am J Physiol* 1995;**268**:F657–F663.
12. Kato J, Kitamura K, Eto T. Plasma adrenomedullin level and development of hypertension. *J Hum Hypertens* 2006;**20**:566–570.
13. Nakamura R, Kato J, Kitamura K, Onitsuka H, Imamura T, Cao Y *et al.* Adrenomedullin administration immediately after myocardial infarction ameliorates progression of heart failure in rats. *Circulation* 2004;**110**: 426–431.
14. Okumura H, Nagaya N, Itoh T, Okano I, Hino J, Mori K *et al.* Adrenomedullin infusion attenuates myocardial ischemia/reperfusion injury through the phosphatidylinositol 3-kinase/Akt-dependent pathway. *Circulation* 2004;**109**:242–248.
15. Kato J, Tsuruda T, Kita T, Kitamura K, Eto T. Adrenomedullin: a protective factor for blood vessels. *Arterioscler Thromb Vasc Biol* 2005;**25**: 2480–2487.
16. Miyashita K, Itoh H, Sawada N, Fukunaga Y, Sone M, Yamahara K *et al.* Adrenomedullin provokes endothelial Akt activation and promotes vascular regeneration both in vitro and in vivo. *FEBS Lett* 2003;**544**:86–92.
17. Kim W, Moon SO, Sung MJ, Kim SH, Lee S, So JN *et al.* Angiogenic role of adrenomedullin through activation of Akt, mitogen-activated protein kinase, and focal adhesion kinase in endothelial cells. *FASEB J* 2003;**17**: 1937–1939.
18. Oehler MK, Fischer DC, Orlowska-Volk M, Herrle F, Kieback DG, Rees MC *et al.* Tissue and plasma expression of the angiogenic peptide adrenomedullin in breast cancer. *Br J Cancer* 2003;**89**:1927–1933.
19. Fritz-Six KL, Dunworth WP, Li M, Caron KM. Adrenomedullin signaling is necessary for murine lymphatic vascular development. *J Clin Invest* 2008;**118**:40–50.
20. Rodriguez-Niedenfuhr M, Papoutsi M, Christ B, Nicolaides KH, von Kaisenberg CS, Tomarev SI *et al.* Prox1 is a marker of ectodermal placodes, endodermal compartments, lymphatic endothelium and lymphangioblasts. *Anat Embryol (Berl)* 2001;**204**:399–406.
21. Nikitenko LL, Blucher N, Fox SB, Bicknell R, Smith DM, Rees MC. Adrenomedullin and CGRP interact with endogenous calcitonin-receptor-like receptor in endothelial cells and induce its desensitisation by different mechanisms. *J Cell Sci* 2006;**119**:910–922.
22. Nishikimi T, Horio T, Yoshihara F, Nagaya N, Matsuo H, Kangawa K. Effect of adrenomedullin on cAMP and cGMP levels in rat cardiac myocytes and nonmyocytes. *Eur J Pharmacol* 1998;**353**:337–344.
23. Boardman KC, Swartz MA. Interstitial flow as a guide for lymphangiogenesis. *Circ Res* 2003;**92**:801–808.
24. Nagaya N, Satoh T, Nishikimi T, Uematsu M, Furuichi S, Sakamaki F *et al.* Hemodynamic, renal, and hormonal effects of adrenomedullin infusion in patients with congestive heart failure. *Circulation* 2000;**101**:498–503.
25. Nagaya N, Nishikimi T, Horio T, Yoshihara F, Kanazawa A, Matsuo H *et al.* Cardiovascular and renal effects of adrenomedullin in rats with heart failure. *Am J Physiol* 1999;**276**:R213–R218.
26. Nagaya N, Kyotani S, Uematsu M, Ueno K, Oya H, Nakanishi N *et al.* Effects of adrenomedullin inhalation on hemodynamics and exercise capacity in patients with idiopathic pulmonary arterial hypertension. *Circulation* 2004;**109**:351–356.
27. Kato J, Kitamura K, Kangawa K, Eto T. Receptors for adrenomedullin in human vascular endothelial cells. *Eur J Pharmacol* 1995;**289**:383–385.
28. Shimekake Y, Nagata K, Ohta S, Kambayashi Y, Teraoka H, Kitamura K *et al.* Adrenomedullin stimulates two signal transduction pathways, cAMP accumulation and Ca^{2+} mobilization, in bovine aortic endothelial cells. *J Biol Chem* 1995;**270**:4412–4417.
29. Yu Y, Sato JD. MAP kinases, phosphatidylinositol 3-kinase, and p70 S6 kinase mediate the mitogenic response of human endothelial cells to vascular endothelial growth factor. *J Cell Physiol* 1999;**178**:235–246.
30. Ilan N, Mahooti S, Madri JA. Distinct signal transduction pathways are utilized during the tube formation and survival phases of in vitro angiogenesis. *J Cell Sci* 1998;**111**:3621–3631.
31. Nagaya N, Mori H, Murakami S, Kangawa K, Kitamura S. Adrenomedullin: angiogenesis and gene therapy. *Am J Physiol Regul Integr Comp Physiol* 2005;**288**:R1432–R1437.
32. Iimuro S, Shindo T, Moriyama N, Amaki T, Niu P, Takeda N *et al.* Angiogenic effects of adrenomedullin in ischemia and tumor growth. *Circ Res* 2004; **95**:415–423.
33. Tokunaga N, Nagaya N, Shirai M, Tanaka E, Ishibashi-Ueda H, Harada-Shiba M *et al.* Adrenomedullin gene transfer induces therapeutic angiogenesis in a rabbit model of chronic hind limb ischemia: benefits of a novel nonviral vector, gelatin. *Circulation* 2004;**109**:526–531.
34. Rutkowski JM, Boardman KC, Swartz MA. Characterization of lymphangiogenesis in a model of adult skin regeneration. *Am J Physiol Heart Circ Physiol* 2006;**291**:H1402–H1410.
35. Meininger CJ, Granger HJ. Mechanisms leading to adenosine-stimulated proliferation of microvascular endothelial cells. *Am J Physiol* 1990;**258**: H198–H206.
36. Fang Y, Olah ME. Cyclic AMP-dependent, protein kinase A-independent activation of extracellular signal-regulated kinase 1/2 following adenosine receptor stimulation in human umbilical vein endothelial cells: role of exchange protein activated by cAMP 1 (Epac1). *J Pharmacol Exp Ther* 2007;**322**:1189–1200.
37. Kitamura K, Sakata J, Kangawa K, Kojima M, Matsuo H, Eto T. Cloning and characterization of cDNA encoding a precursor for human adrenomedullin. *Biochem Biophys Res Commun* 1993;**194**:720–725.
38. Okazaki T, Ogawa Y, Tamura N, Mori K, Isse N, Aoki T *et al.* Genomic organization, expression, and chromosomal mapping of the mouse adrenomedullin gene. *Genomics* 1996;**37**:395–399.
39. Ashton D, Hieble P, Gout B, Alyar N. Vasodilatory effect of adrenomedullin in mouse aorta. *Pharmacology* 2000;**61**:101–105.
40. Tonnesen MG, Feng X, Clark RA. Angiogenesis in wound healing. *J Investig Dermatol Symp Proc* 2000;**5**:40–46.
41. Hirakawa S, Detmar M. New insights into the biology and pathology of the cutaneous lymphatic system. *J Dermatol Sci* 2004;**35**:1–8.
42. Jeltsch M, Kaipainen A, Joukov V, Meng X, Lakso M, Rauvala H *et al.* Hyperplasia of lymphatic vessels in VEGF-C transgenic mice. *Science* 1997;**276**:1423–1425.
43. Cao R, Eriksson A, Kubo H, Alitalo K, Cao Y, Thyberg J. Comparative evaluation of FGF-2-, VEGF-A-, and VEGF-C-induced glogenesis, lymphangiogenesis, vascular fenestrations, and permeability. *Circ Res* 2004;**94**: 664–670.

FEBS Letters 581 (2007) 3961–3966

Mesenchymal stem cells attenuate cardiac fibroblast proliferation and collagen synthesis through paracrine actions

Shunsuke Ohnishi[a,*], Hideaki Sumiyoshi[b], Soichiro Kitamura[c], Noritoshi Nagaya[a,*]

[a] Department of Regenerative Medicine and Tissue Engineering, National Cardiovascular Center Research Institute, 5-7-1 Fujishirodai, Osaka 565-8565, Japan
[b] Department of Anatomy, Biology and Medicine, Faculty of Medicine, Oita University, Oita, Japan
[c] Department of Cardiovascular Surgery, National Cardiovascular Center, Osaka, Japan

Received 2 July 2007; accepted 12 July 2007

Available online 23 July 2007

Edited by Veli-Pekka Lehto

Abstract **Mesenchymal stem cells (MSC) transplantation has been shown to decrease fibrosis in the heart; however, whether MSC directly influence the function of cardiac fibroblasts (CFB) remains unknown. MSC-conditioned medium significantly attenuated proliferation of CFB compared with CFB-conditioned medium. MSC-conditioned medium upregulated antiproliferation-related genes such as elastin, myocardin and DNA-damage inducible transcript 3, whereas CFB-conditioned medium upregulated proliferation-related genes such as alpha-2-macrogrobulin and v-kit Hardy–Zuckerman 4 feline sarcoma viral oncogene homolog. MSC-conditioned medium significantly downregulated type I and III collagen expression, and significantly suppressed type III collagen promoter activity. MSC may exert paracrine anti-fibrotic effects at least in part through regulation of CFB proliferation and collagen synthesis.**
© 2007 Federation of European Biochemical Societies. Published by Elsevier B.V. All rights reserved.

Keywords: Mesenchymal stem cell; Cardiac fibroblast; Cell proliferation; Collagen; Paracrine effect; Collagenase activity

1. Introduction

Mesenchymal stem cells (MSC) can differentiate into a variety of cell types including cardiomyocytes and vascular endothelial cells, and can be easily isolated from bone marrow and expanded in culture [1]. These features make MSC an attractive therapeutic tool for cardiovascular disease. We and others have previously demonstrated that MSC transplantation caused significant improvement in hindlimb ischemia [2], myocardial infarction [3,4], dilated cardiomyopathy [5] and acute myocarditis [6]. MSC transplantation has been shown to result in cardiac repair and protection at least in part through paracrine actions such as angiogenic, anti-apoptotic, and anti-inflammatory effects [2,3,5–10]. In addition, it has been demonstrated in animal models that MSC transplantation decreases fibrosis in the heart [5] and other organs such as lung [11,12], liver [13,14] and kidney [15]. However, whether transplanted MSC directly influence the function of cardiac fibroblasts (CFB) remains unknown.

Deposition of collagen fibers in the myocardial interstitium occurs in the remodeling process seen in a variety of cardiovascular diseases, and CFB are predominantly involved in the maintenance of extracellular matrix such as types I and III collagen by cell proliferation, collagen synthesis and degradation [16]. Collagen synthesis is regulated by fibrogenic factors, and collagen degradation is mediated by members of the matrix metalloproteinases (MMPs), which are also regulated by tissue inhibitors of metalloproteinases [17,18].

Thus, we investigated the paracrine effects of MSC on (1) CFB proliferation, (2) collagen synthesis and (3) collagen degradation in vitro.

2. Materials and methods

2.1. Cell culture and collection of conditioned medium

Isolation and expansion of MSC were performed as described previously [2]. Briefly, bone marrow cells were isolated from male Lewis rats weighing 220–250 g by flushing out the femoral and tibial cavities with phosphate-buffered saline, and cultured in standard medium: α-minimal essential medium, 10% fetal bovine serum, 100 U/ml penicillin and 100 μg/ml streptomycin. Five days after plating, non-adherent cells were removed, and adherent cells were further propagated for 4–5 passages. These cells were previously demonstrated to be positive for CD29 and CD90 surface markers, and negative for CD34 and CD45 [5]. The Animal Care Committee of the National Cardiovascular Center approved the experimental protocol.

Primary CFB were obtained as described previously with modification [19]. Briefly, after heparinization by intraperitoneal injection of 1000 U/kg heparin sodium, the heart was rapidly excised, and pulmonary, connective and other non-cardiac tissues were removed. The heart was then mounted on the cannula of a modified Langendorff apparatus and perfused with buffer containing 0.75 mg/ml collagenase type I (Worthington, Lakewood, NJ), 0.5 mg/ml hyaluronidase (Sigma–Aldrich, St. Louis, MO) and 1% bovine serum albumin (fraction V, ICN, Aurora, OH), in a recirculating fashion for 3 h. After perfusion, the heart was removed from the perfusion apparatus, and the atrium was removed and gently minced. CFB were gravitationally separated from cardiomyocytes, and cultured in standard medium.

Conditioned medium was collected from MSC and CFB after the second passage of 3×10^5 cells cultured in standard medium for 48 h, and filtered through a 0.22 μm-filtration unit (Millipore, Bedford, MA).

*Corresponding authors. Fax: +81 6 6833 9865.
E-mail addresses: sonishi@ri.ncvc.go.jp (S. Ohnishi), nnagaya@ri.ncvc.go.jp (N. Nagaya).

Abbreviations: MSC, mesenchymal stem cell; CFB, cardiac fibroblast; MMP, matrix metalloproteinase; qRT-PCR, quantitative real-time reverse-transcription polymerase chain reaction; Gapdh, glyceraldehyde 3-phosphate dehydrogenase; A2m, alpha-2-macroglobulin; Kit, v-kit Hardy–Zuckerman 4 feline sarcoma viral oncogene homolog; Catna1, catenin alpha 1; Rarb, retinoic acid receptor beta; Eln, elastin; Myocd, myocardin; Ddit3, DNA-damage inducible transcript 3

0014-5793/$32.00 © 2007 Federation of European Biochemical Societies. Published by Elsevier B.V. All rights reserved.
doi:10.1016/j.febslet.2007.07.028

2.2. MTS assay

We investigated the paracrine effects of MSC on fibroblast proliferation in vitro. Experiments were carried out using cells derived from five passages. CFB were plated on 96-well plates (4×10^3 cells/well). After 24 h, the medium was changed to conditioned medium obtained from MSC or CFB culture for 48 h. After 48 h, the cellular level of 3-(4,5-dimethylthiazol-2-yl)-5-(3-carboxymethoxyphenyl)-2-(4- sulfophenyl)-2H-tetrazolium (MTS), indicative of the mitochondrial function of living cells and cell viability, was measured with a CellTiter96 AQueous One Solution Kit (Promega, Madison, WI) and a Microplate Reader (490 nm, Bio-Rad, Hercules, CA).

2.3. Microarray analysis

Total RNA was extracted from cells using an RNeasy Mini Kit (Qiagen, Hilden, Germany) according to the manufacturer's instructions. RNA was quantified by spectrometry and the quality confirmed by gel electrophoresis. Microarray analysis was performed as described previously [20]. In brief, double-stranded cDNA was synthesized from 4 μg total RNA, and in vitro transcription was performed to produce biotin-labeled cRNA using GeneChip One-Cycle Target Labeling and Control Reagents (Affymetrix, Santa Clara, CA) according to the manufacturer's instructions. After fragmentation, 10 μg cRNA was hybridized with GeneChip Rat Genome 230 2.0 Array (Affymetrix) containing 31099 genes. GeneChips were then scanned in a GeneChip Scanner 3000 (Affymetrix). Normalization, filtering, and Gene Ontology analysis of the data were performed with GeneSpring GX 7.3.1 software (Agilent Technologies, Palo Alto, CA). The raw data from each array were normalized as follows; each CEL file was preprocessed with Robust Multichip Average (RMA), and each measurement for each gene was divided by the 80th percentile of all measurements. Genes with an at least 1.8-fold change were then selected.

2.4. Quantitative real-time reverse-transcription polymerase chain reaction (qRT-PCR)

One microgram of total RNA was reverse-transcribed into cDNA using a Quantitect Reverse Transcription Kit (Qiagen). PCR amplification was performed in 50 μl containing 1 μl cDNA and 25 μl Power SYBR Green PCR Master Mix (Applied Biosystems, Foster City, CA). Glyceraldehyde 3-phosphate dehydrogenase (Gapdh) mRNA amplified from the same samples served as an internal control. Primers used in qRT-PCR analysis were as follows: Col1a1: forward, 5′-TCAAGATGGTGGCCGTTAC-3′, reverse, 5′-CTGCGGATGTTC-TCAATCTG-3′, Col3a1: forward, 5′-CGAGATTAAAGCAAGAGGAA-3′, reverse, 5′-GAGGCTTCTTTACATACCAC-3′, Gapdh: forward, 5′-TGAAGGTCGGTGTCAACGGATTTGGC-3′, reverse, 5′-CATGTAGGCCATGAGGTCCACCAC-3′. After an initial denaturation at 95°C for 10 min, a two-step cycle procedure was used (denaturation at 95 °C for 15 s, annealing and extension at 60 °C for 1 min) for 40 cycles in a 7700 sequence detector (Applied Biosystems). Gene expression levels were normalized according to that of Gapdh. The data were analyzed with Sequence Detection Systems software (Applied Biosystems).

2.5. Transient transfection and reporter gene assay

Transient transfection and subsequent reporter gene assay were performed as described previously with modification [21]. The Col1a1 clones containing the promoter fragments −1685/+68Luc and −96/+68Luc were provided by Dr. H. Yoshioka of Oita University, Japan. CFB were plated at a density of 1×10^4 cells in 96-well plates with 100 μl culture medium. After incubation for 24 h at 37 °C, cells were transfected with 200 ng luciferase plasmid DNA plus 10 ng Renilla phRL-TK vector (Promega, Madison, WI) as an internal control, using lipofectamine2000 (Invitrogen). Six hours after transfection, cells were rinsed with PBS, fed with conditioned medium obtained from MSC or CFB culture, and then further cultured for 48 h. Reporter gene assay was performed using the Dual-Glo Luciferase reporter assay system (Promega), and the luminescence intensity was measured using a microplate reader (Dia-Iatron, Tokyo, Japan), according to the manufacturer's protocol. The transcription activity was normalized according to Renilla luciferase activity.

2.6. Collagenase activity

Collagenase activity assay was performed using a collagenase assay kit (Chondrex, Redmond, WA) following the manufacturer's instructions. CFB were cultured in CFB- or MSC-conditioned medium with fluorescein isothiocyanate-labeled type I collagen for 48 h, and degraded collagen was extracted by denaturation, proteinase treatment and centrifugation. Fluorescence intensity was measured using a fluorometer (Tecan, Salzburg, Austria) at excitation/emission of 485/535 nm.

2.7. Statistical analysis

Data were expressed as means ± standard error (S.E.). Comparisons of parameters among groups were made by one-way ANOVA, followed by Newman–Keuls' test. Differences were considered significant at $P < 0.05$.

3. Results

3.1. Effect of MSC-conditioned medium on proliferation of CFB

To investigate the effect of MSC-conditioned medium on CFB proliferation, we cultured CFB in standard medium, CFB- or MSC-conditioned medium for 48 h, and MTS assay was performed. Viable cell number was significantly larger when CFB were cultured in CFB-conditioned medium compared with standard medium, whereas this increase was not observed when CFB were cultured in MSC-conditioned medium (Fig. 1A, B). These results suggest that MSC attenuates proliferation of CFB through paracrine actions.

3.2. Effect of MSC-conditioned medium on expression of genes involved in cell proliferation in CFB

We next performed microarray analysis to examine the effect of MSC-conditioned medium on the expression of genes involved in the regulation of cell proliferation in CFB. Highly expressed genes in CFB cultured in CFB-conditioned medium (>1.8-fold) included positive regulators for cell proliferation such as alpha-2-macroglobulin (A2m) and v-kit Hardy–Zuckerman 4 feline sarcoma viral oncogene homolog (Kit), as well as negative regulators for cell proliferation such as catenin alpha 1 (Catna1) and retinoic acid receptor beta (Rarb). On the other hand, CFB cultured in MSC-conditioned medium highly expressed negative regulators for cell proliferation such as elastin (Eln), myocardin (Myocd) and DNA-damage inducible transcript 3 (Ddit3) (Table 1).

3.3. Effect of MSC-conditioned medium on collagen gene expression

To investigate the effect of MSC-conditioned medium on collagen gene expression, we performed qRT-PCR on types I and III collagen genes (Col1a1 and Col3a1, respectively) in CFB. Expression of Col1a1 and Col3a1 genes was significantly upregulated when CFB were cultured in CFB-conditioned medium in comparison to standard medium. However, this increase was significantly attenuated when CFB were cultured in MSC-conditioned medium (Fig. 2A, B).

3.4. Effect of MSC-conditioned medium on collagen gene promoter activity

To investigate the effect of MSC-conditioned medium on Col3a1 gene promoter activity, we performed reporter gene assay in CFB. We prepared −1685/+68Luc and −96/+68Luc constructs (Fig. 3A), as the −96 to −34 region has been reported to be fundamental for Col3a1 gene transcription [21]. The activity of −1685/+68Luc was significantly higher in

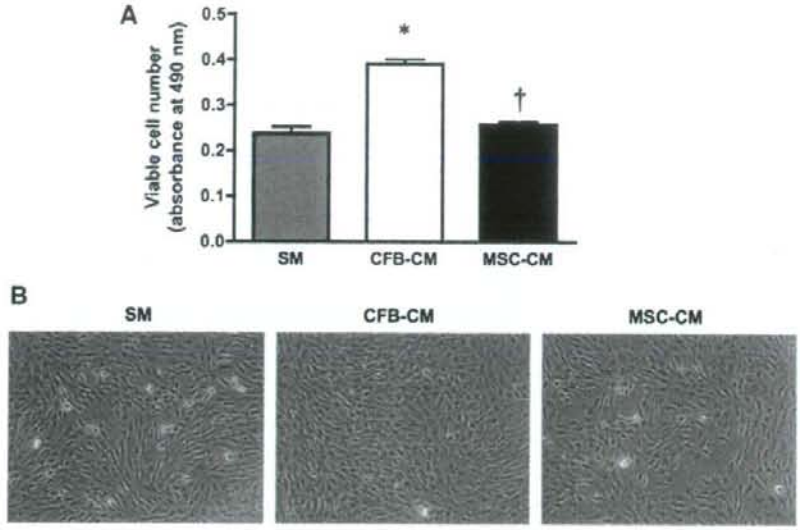

Fig. 1. Effect of MSC-conditioned medium on CFB proliferation MTS assay (A) and representative photographs (B) of CFB after 48 h of culture in the indicated medium. SM, standard medium; CM, conditioned medium. Values are means ± S.E. $^{*}P < 0.05$ vs SM, $^{\dagger}P < 0.05$ vs CFB-CM.

Table 1
Expression of genes involved in regulation of cell proliferation (>1.8-fold)

Gene name	Action on cell proliferation	Fold change
Genes highly expressed in CFB-conditioned medium		
catenin, alpha 1 (Catna1)	Neg	2.3
retinoic acid receptor, beta (Rarb)	Neg	2.1
alpha-2-macroglobulin (A2m)	Pos	2.0
v-kit Hardy–Zuckerman 4 feline sarcoma viral oncogene homolog (Kit)	Pos	1.8
Genes highly expressed in MSC-conditioned medium		
elastin (Eln)	Neg	3.8
myocardin (Myocd)	Neg	1.9
DNA-damage inducible transcript 3 (Ddit3)	Neg	1.8

CFB-conditioned medium as compared to standard medium, whereas it was markedly decreased in MSC-conditioned medium (Fig. 3B). However, the activity of −96/+68Luc was not affected in either CFB- or MSC-conditioned medium. These results suggest that MSC-conditioned medium inhibits Col3a1 gene transcription through regulation of the −1685 to −96 promoter region.

3.5. Effect of MSC-conditioned medium on collagenase activity

We finally investigated the effect of MSC-conditioned medium on collagen degradation. Type I collagenase activity was markedly higher in CFB-conditioned medium than in standard medium; however, MSC-conditioned medium had as high collagenase activity as CFB-conditioned medium (Fig. 4).

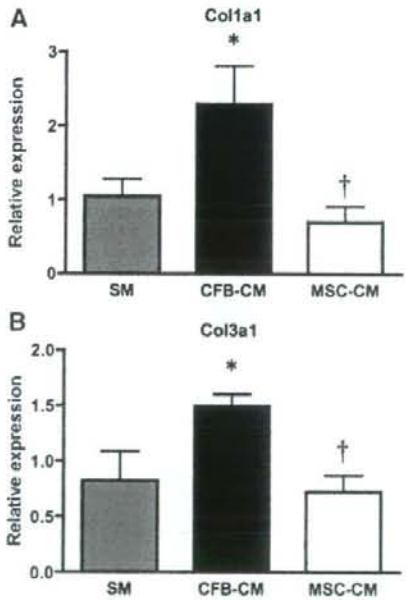

Fig. 2. Effect of MSC-conditioned medium on collagen gene expression (A) Quantitative RT-PCR for Col1a1 expression in CFB after 48 h of culture in the indicated medium. (B) Quantitative RT-PCR for Col3a1 expression in CFB after 48 h of culture in the indicated medium. SM, standard medium; CM, conditioned medium. Values are means ± S.E. $^{*}P < 0.05$ vs SM, $^{\dagger}P < 0.05$ vs CFB-CM.

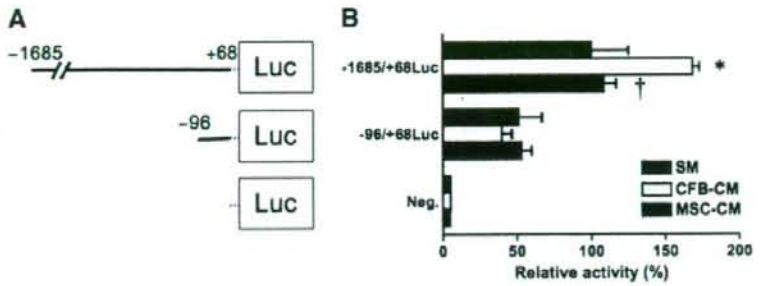

Fig. 3. Effect of MSC-conditioned medium on type III collagen gene promoter activity (A) Schematic illustration of 5′-deletion constructs of the Col3a1 promoter. (B) Luficerase activity in CFB after 48 hours of transfection of reporter plasmids and culture in the indicated medium. All constructs were co-transfected with the phRL-TK vector as an internal control for transfection efficiency. SM, standard medium; CM, conditioned medium. Values are means ± S.E. $^{*}P < 0.05$ vs SM, $^{\dagger}P < 0.05$ vs CFB-CM.

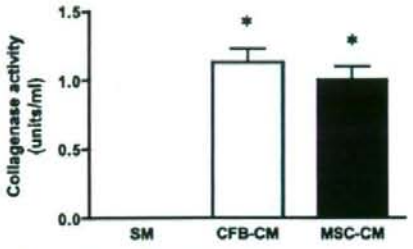

Fig. 4. Effect of MSC-conditioned medium on collagenase activity Type I collagenase activity of the indicated medium. SM, standard medium; CM, conditioned medium. Values are means ± S.E. $^{*}P < 0.05$ vs SM.

4. Discussion

In this study, we focused on the paracrine effects of MSC on CFB in vitro, and demonstrated that MSC-conditioned medium: (1) attenuated CFB proliferation, (2) regulated expression of several genes involved in CFB proliferation, (3) transcriptionally inhibited type I and III collagen gene expression in CFB, and (4) had comparable collagenase activity to that of CFB-conditioned medium.

We and others have previously demonstrated that MSC mediate pleiotropic effects by secreting a large number of growth factors, anti-apoptotic factors and cytokines [2,3,5–10]. In addition, we have recently reported that MSC transplantation improved cardiac function at least in part through an anti-fibrotic effect in a rat model of dilated cardiomyopathy and acute myocarditis [5,6], and also demonstrated that the highly expressed genes in cultured MSC included a number of molecules involved in biogenesis of extracellular matrix such as collagens, MMPs, serine proteases and serine protease inhibitors [20]. These results suggest that transplanted MSC may inhibit the fibrogenic process through paracrine actions.

In the present study, CFB proliferation was slower when they were cultured in MSC-conditioned medium than in CFB-conditioned medium, and microarray analysis demonstrated that the expression levels of several genes involved in cell proliferation were differently regulated. Out of four highly expressed genes in CFB cultured in CFB-conditioned medium, two genes (A2m and Kit) are known to positively regulate cell proliferation, whereas the other two genes (Catna1 and Rarb) are known to be negative regulators. Catna1 encodes α-catenin which interacts with cadherin, a cell adhesion molecule, and targeted deletion of Catna1 in either the skin or in neuronal progenitor cells leads to hyperproliferation [22]. Rarb encodes a member of retinoic acid receptors, and regulated cell growth and differentiation in a variety of cells [23]. A2m encodes a plasma proteinase inhibitor [24], and induces macrophage proliferation through cAMP-dependent signaling [25]. Kit encodes c-kit protein, a tyrosine kinase receptor for stem cell factor, and ectopic expression of c-kit in fibroblasts induces tumorigenesis [26]. On the other hand, three negative regulators of cell proliferation were upregulated in CFB cultured in MSC-conditioned medium. Eln encodes a polymer of a precursor protein (tropoelastin), and impaired elastogenesis coincides with increased cell proliferation [27]. Mycd encodes a transcription factor important for smooth muscle and cardiac muscle development, and inactivation of Mycd in fibroblasts increases their proliferative potential [28]. Ddit3 belongs to the CCAAT/enhancer binding protein family of transcription factors, and exogenous Ddit3 is capable of inducing growth arrest and apoptosis [29]. Taking these findings together, MSC may negatively regulate CFB proliferation by controlling these factors, although the precise mechanism remains to be elucidated.

Types I and III collagen are the major fibrillar collagen produced by CFB, and the expression of collagen genes is regulated at the transcriptional and post-transcriptional levels [30]. It has been suggested that an initial mesh of type III collagen forms the scaffold for subsequent deposition of large, highly aligned type I collagen fibers at the fibrotic phase after myocardial infarction [31]. In the present study, the expression of Col1a1 as well as Col3a1 was downregulated when CFB were cultured in MSC-conditioned medium. This result is consistent with a recent study by Guo et al., which demonstrated that MSC transplantation in a rat model of myocardial infarction inhibited deposition of types I and III collagen [32]. Although the transcriptional mechanism of the Col3a1 gene is not entirely characterized, our in vitro experiments suggest that, in comparison to CFB-conditioned medium, MSC-conditioned medium may be rich in humoral factors that can inactivate transcription, or poor in humoral factors that can activate transcription, of Col3a1.

Collagenase (MMP-1) and gelatinase (MMP-2 and -9) activity are known to be elevated during the necrotic phase of infarct healing, and are involved in disruption of the collagen network [33]. In the present study, type I collagenase activity of MSC-conditioned medium was as high as that of CFB-conditioned medium. Type I collagen is a substrate for MMP-1, -2, -8 and -13, and the mechanisms involved in the differential regulation of the various collagen types during cardiac fibrosis appear to be complex and diverse [34]. However, our results imply that MSC have equivalent paracrine effects on type I collagenase activity to those of CFB.

In conclusion, MSC exerted paracrine anti-fibrotic effects at least in part through regulation of CFB proliferation and transcriptional downregulation of types I and III collagen syntheses. These features of MSC may be beneficial for the treatment of heart failure in which fibrotic changes are involved.

Acknowledgements: This work was supported by research grants for Cardiovascular Disease (18C-1 and 19C-7) and Human Genome Tissue Engineering 009 from the Ministry of Health, Labour and Welfare, and by the Japan Vascular Disease Research Foundation.

References

[1] Pittenger, M.F. and Martin, B.J. (2004) Mesenchymal stem cells and their potential as cardiac therapeutics. Circ. Res. 95, 9–20.
[2] Iwase, T., Nagaya, N., Fujii, T., Itoh, T., Murakami, S., Matsumoto, T., Kangawa, K. and Kitamura, S. (2005) Comparison of angiogenic potency between mesenchymal stem cells and mononuclear cells in a rat model of hindlimb ischemia. Cardiovasc. Res. 66, 543–551.
[3] Miyahara, Y., Nagaya, N., Kataoka, M., Yanagawa, B., Tanaka, K., Hao, H., Ishino, K., Ishida, H., Shimizu, T., Kangawa, K., Sano, S., Okano, T., Kitamura, S. and Mori, H. (2006) Monolayered mesenchymal stem cells repair scarred myocardium after myocardial infarction. Nat. Med. 12, 459–465.
[4] Abdel-Latif, A., Bolli, R., Tleyjeh, I.M., Montori, V.M., Perin, E.C., Hornung, C.A., Zuba-Surma, E.K., Al-Mallah, M. and Dawn, B. (2007) Adult bone marrow-derived cells for cardiac repair: a systematic review and meta-analysis. Arch. Intern. Med. 167, 989–997.
[5] Nagaya, N., Kangawa, K., Itoh, T., Iwase, T., Murakami, S., Miyahara, Y., Fujii, T., Uematsu, M., Ohgushi, H., Yamagishi, M., Tokudome, T., Mori, H., Miyatake, K. and Kitamura, S. (2005) Transplantation of mesenchymal stem cells improves cardiac function in a rat model of dilated cardiomyopathy. Circulation 112, 1128–1135.
[6] Ohnishi, S., Yanagawa, B., Tanaka, K., Miyahara, Y., Obata, H., Kataoka, M., Kodama, M., Ishibashi-Ueda, H., Kangawa, K., Kitamura, S. and Nagaya, N. (2007) Transplantation of mesenchymal stem cells attenuates myocardial injury and dysfunction in a rat model of acute myocarditis. J. Mol. Cell Cardiol. 42, 88–97.
[7] Kinnaird, T., Stabile, E., Burnett, M.S., Lee, C.W., Barr, S., Fuchs, S. and Epstein, S.E. (2004) Marrow-derived stromal cells express genes encoding a broad spectrum of arteriogenic cytokines and promote in vitro and in vivo arteriogenesis through paracrine mechanisms. Circ. Res. 94, 678–685.
[8] Kinnaird, T., Stabile, E., Burnett, M.S., Shou, M., Lee, C.W., Barr, S., Fuchs, S. and Epstein, S.E. (2004) Local delivery of marrow-derived stromal cells augments collateral perfusion through paracrine mechanisms. Circulation 109, 1543–1549.
[9] Gnecchi, M., He, H., Liang, O.D., Melo, L.G., Morello, F., Mu, H., Noiseux, N., Zhang, L., Pratt, R.E., Ingwall, J.S. and Dzau, V.J. (2005) Paracrine action accounts for marked protection of ischemic heart by Akt-modified mesenchymal stem cells. Nat. Med. 11, 367–368.
[10] Gnecchi, M., He, H., Noiseux, N., Liang, O.D., Zhang, L., Morello, F., Mu, H., Melo, L.G., Pratt, R.E., Ingwall, J.S. and Dzau, V.J. (2006) Evidence supporting paracrine hypothesis for Akt-modified mesenchymal stem cell-mediated cardiac protection and functional improvement. FASEB J. 20, 661–669.
[11] Ortiz, L.A., Gambelli, F., McBride, C., Gaupp, D., Baddoo, M., Kaminski, N. and Phinney, D.G. (2003) Mesenchymal stem cell engraftment in lung is enhanced in response to bleomycin exposure and ameliorates its fibrotic effects. Proc. Natl. Acad. Sci. USA 100, 8407–8411.
[12] Rojas, M., Xu, J., Woods, C.R., Mora, A.L., Spears, W., Roman, J. and Brigham, K.L. (2005) Bone marrow-derived mesenchymal stem cells in repair of the injured lung. Am. J. Respir. Cell Mol. Biol. 33, 145–152.
[13] Oyagi, S., Hirose, M., Kojima, M., Okuyama, M., Kawase, M., Nakamura, T., Ohgushi, H. and Yagi, K. (2006) Therapeutic effect of transplanting HGF-treated bone marrow mesenchymal cells into CCl4-injured rats. J. Hepatol. 44, 742–748.
[14] Abdel Aziz, M.T., Atta, H.M., Mahfouz, S., Fouad, H.H., Roshdy, N.K., Ahmed, H.H., Rashed, L.A., Sabry, D., Hassouna, A.A. and Hasan, N.M. (2007) Therapeutic potential of bone marrow-derived mesenchymal stem cells on experimental liver fibrosis. Clin. Biochem. 40, 893–899.
[15] Ninichuk, V., Gross, O., Segerer, S., Hoffmann, R., Radomska, E., Buchstaller, A., Huss, R., Akis, N., Schlondorff, D. and Anders, H.J. (2006) Multipotent mesenchymal stem cells reduce interstitial fibrosis but do not delay progression of chronic kidney disease in collagen4A3-deficient mice. Kidney Int. 70, 121–129.
[16] Brown, R.D., Ambler, S.K., Mitchell, M.D. and Long, C.S. (2005) The cardiac fibroblast: therapeutic target in myocardial remodeling and failure. Annu. Rev. Pharmacol. Toxicol. 45, 657–687.
[17] Jugdutt, B.I. (2003) Remodeling of the myocardium and potential targets in the collagen degradation and synthesis pathways. Curr. Drug Targets Cardiovasc. Haematol. Disord. 3, 1–30.
[18] Lijnen, P.J. and Petrov, V.V. (2003) Role of intracardiac renin–angiotensin–aldosterone system in extracellular matrix remodeling. Methods Find. Exp. Clin. Pharmacol. 25, 541–564.
[19] Tanaka, K., Honda, M. and Takabatake, T. (2001) Redox regulation of MAPK pathways and cardiac hypertrophy in adult rat cardiac myocyte. J. Am. Coll. Cardiol. 37, 676–685.
[20] Ohnishi, S., Yasuda, T., Kitamura, S. and Nagaya, N. (2007) Effect of hypoxia on gene expression of bone marrow-derived mesenchymal stem cells and mononuclear cells. Stem Cells 25, 1166–1177.
[21] Yoshino, T., Sumiyoshi, H., Shin, T., Matsuo, N., Inagaki, Y., Ninomiya, Y. and Yoshioka, H. (2005) Multiple proteins are involved in the protein-DNA complex in the proximal promoter of the human alpha1(III) collagen gene (COL3A1). Biochim. Biophys. Acta 1729, 94–104.
[22] Vasioukhin, V., Bauer, C., Degenstein, L., Wise, B. and Fuchs, E. (2001) Hyperproliferation and defects in epithelial polarity upon conditional ablation of alpha-catenin in skin. Cell 104, 605–617.
[23] Chambon, P. (1994) The retinoid signaling pathway: molecular and genetic analyses. Semin. Cell Biol. 5, 115–125.
[24] Baker, A.H., Edwards, D.R. and Murphy, G. (2002) Metalloproteinase inhibitors: biological actions and therapeutic opportunities. J. Cell Sci. 115, 3719–3727.
[25] Misra, U.K., Akabani, G. and Pizzo, S.V. (2002) The role of cAMP-dependent signaling in receptor-recognized forms of alpha 2-macroglobulin-induced cellular proliferation. J. Biol. Chem. 277, 36509–36520.
[26] Caruana, G., Cambareri, A.C., Gonda, T.J. and Ashman, L.K. (1998) Transformation of NIH3T3 fibroblasts by the c-Kit receptor tyrosine kinase: effect of receptor density and ligand-requirement. Oncogene 16, 179–190.
[27] Urban, Z., Riazi, S., Seidl, T.L., Katahira, J., Smoot, L.B., Chitayat, D., Boyd, C.D. and Hinek, A. (2002) Connection between elastin haploinsufficiency and increased cell proliferation in patients with supravalvular aortic stenosis and Williams–Beuren syndrome. Am. J. Hum. Genet. 71, 30–44.
[28] Milyavsky, M., Shats, I., Cholostoy, A., Brosh, R., Buganim, Y., Weisz, L., Kogan, I., Cohen, M., Shatz, M., Madar, S., Kalo, E., Goldfinger, N., Yuan, J., Ron, S., MacKenzie, K., Eden, A. and Rotter, V. (2007) Inactivation of myocardin and p16 during malignant transformation contributes to a differentiation defect. Cancer Cell 11, 133–146.

[29] Maytin, E.V., Ubeda, M., Lin, J.C. and Habener, J.F. (2001) Stress-inducible transcription factor CHOP/gadd153 induces apoptosis in mammalian cells via p38 kinase-dependent and -independent mechanisms. Exp. Cell Res. 267, 193–204.
[30] Ghosh, A.K. (2002) Factors involved in the regulation of type I collagen gene expression: implication in fibrosis. Exp. Biol. Med. (Maywood) 227, 301–314.
[31] Whittaker, P., Boughner, D.R. and Kloner, R.A. (1989) Analysis of healing after myocardial infarction using polarized light microscopy. Am. J. Pathol. 134, 879–893.
[32] Guo, J., Lin, G.S., Bao, C.Y., Hu, Z.M. and Hu, M.Y. (2007) Anti-inflammation role for mesenchymal stem cells transplantation in myocardial infarction. Inflammation 30, 97–104.
[33] Cleutjens, J.P., Kandala, J.C., Guarda, E., Guntaka, R.V. and Weber, K.T. (1995) Regulation of collagen degradation in the rat myocardium after infarction. J. Mol. Cell Cardiol. 27, 1281–1292.
[34] Bishop, J.E. and Lindahl, G. (1999) Regulation of cardiovascular collagen synthesis by mechanical load. Cardiovasc. Res. 42, 27–44.

ELSEVIER

Cardiovascular Research 76 (2007) 110–118

Cardiovascular Research

www.elsevier.com/locate/cardiores

Infusion of adrenomedullin improves acute myocarditis *via* attenuation of myocardial inflammation and edema

Bobby Yanagawa [a,1], Masaharu Kataoka [a,1], Shunsuke Ohnishi [a,*,1], Makoto Kodama [b], Koichi Tanaka [a], Yoshinori Miyahara [a], Hatsue Ishibashi-Ueda [c], Yoshifusa Aizawa [b], Kenji Kangawa [d], Noritoshi Nagaya [a,*]

[a] *Department of Regenerative Medicine and Tissue Engineering, National Cardiovascular Center Research Institute, Osaka, Japan*
[b] *Division of Cardiology, Niigata University Graduate School of Medical and Dental Sciences, Niigata, Japan*
[c] *Department of Pathology, National Cardiovascular Center, Osaka, Japan*
[d] *Department of Biochemistry, National Cardiovascular Center Research Institute, Osaka, Japan*

Received 23 January 2006; received in revised form 7 May 2007; accepted 24 May 2007
Available online 6 June 2007
Time for primary review 23 days

Abstract

Objective: Our aim was to assess whether adrenomedullin (AM), a potent vasodilator peptide with a variety of cardioprotective effects, has a therapeutic potential for the treatment of acute myocarditis in a rat model.
Methods: One week after myosin injection, rats received a continuous infusion of AM or vehicle for 2 weeks, and pathological and physiological investigations were performed.
Results: AM treatment significantly reduced the infiltration of inflammatory cells in myocarditic hearts, and decreased the expressions of macrophage chemoattractant protein-1, matrix metalloproteinase-2 and transforming growth factor-β. Myocardial edema indicated by increased heart weight to body weight ratio and wall thickness was attenuated by AM infusion (5.7±0.5 *vs.* 6.5±0.4 g/kg, and 1.9±0.3 *vs.* 2.8±0.5 mm, respectively). Infusion of AM significantly improved left ventricular maximum d*P*/d*t* and fractional shortening of myocarditic hearts (4203±640 *vs.* 3450±607 mm Hg/s, and 21.3±4.1 *vs.* 14.7±5.1%, respectively).
Conclusion: Infusion of AM improved cardiac function and pathological findings in a rat model of acute myocarditis. Thus, infusion of AM may be a potent therapeutic strategy for acute myocarditis.
© 2007 European Society of Cardiology. Published by Elsevier B.V. All rights reserved.

Keywords: Autoimmune myocarditis; Adrenomedullin; Angiogenesis; Inflammation

1. Introduction

Acute myocarditis is a non-ischemic heart disease characterized by myocardial inflammation and edema. This disease is associated with rapidly progressive heart failure, arrhythmias and sudden death [1]. Although early evidence for efficacy of immunoglobulin and interferon therapy appears promising, these results have yet to be demonstrated in randomized or controlled clinical trials [2]. Current therapeutic options are restricted to supportive care for heart failure or arrhythmias [3]. The lack of specific treatment and the potential severity of the illness emphasize the importance of novel and effective therapeutic strategies for myocarditis.

Adrenomedullin (AM) is a potent vasodilator peptide that was originally isolated from human pheochromocytoma [4]. Earlier studies have shown that AM has beneficial hemodynamic effects on failing hearts *via* its vasodilatory action and diuretic effects [5,6]. Furthermore, AM has direct cardioprotective effects such as anti-inflammatory effects [7], inhibition

* Corresponding authors. Department of Regenerative Medicine and Tissue Engineering, National Cardiovascular Center Research Institute, 5-7-1 Fujishirodai, Suita, Osaka 565-8565, Japan. Tel.: +81 6 6833 5012; fax: +81 6 6835 5496.
E-mail addresses: sonishi@ri.ncvc.go.jp (S. Ohnishi), nnagaya@ri.ncvc.go.jp (N. Nagaya).
[1] These authors contributed equally to this work.

0008-6363/$ - see front matter © 2007 European Society of Cardiology. Published by Elsevier B.V. All rights reserved.
doi:10.1016/j.cardiores.2007.05.027

of apoptosis [8], induction of angiogenesis [9] and attenuation of myocardial hypertrophy [10]. Interestingly, AM has also been shown to decrease endothelial hyperpermeability in the heart [11]. These findings raise the possibility that infusion of AM may attenuate myocardial inflammation and edema in acute myocarditis. Although previous findings have demonstrated that infusion of AM is effective for heart failure, its therapeutic effects in acute myocarditis are still unknown.

Experimental autoimmune myocarditis can be induced in rats by immunizing them with cardiac myosin, providing a model that resembles human giant cell myocarditis [12,13]. Although the majority of acute myocarditis is linked to a viral infection such as coxsackievirus B3, this viral infection can in some cases cause an autoimmune myocarditis with chronic myocardial inflammation without viral persistence, due to the exposure of autoantigens such as cardiac myosin to the immune system [14,15].

Thus, the purposes of this study were 1) to investigate whether infusion of AM improves cardiac function and pathological findings including myocardial inflammation and edema in rats with myosin-induced myocarditis, and 2) to investigate the underlying mechanisms responsible for the effects of AM.

2. Methods

2.1. Experimental autoimmune myocarditis

Purified cardiac myosin from the ventricular muscle of pig hearts was prepared according to a procedure described previously [16]. The antigen was dissolved at a concentration of 20 mg/ml in phosphate-buffered saline (PBS) containing 0.3 M KCl mixed with an equal volume of complete Freund's adjuvant (CFA) containing 11 mg/ml of *Mycobacterium tuberculosis* (Difco Laboratories, Sparks, MD, USA).

Male 10-week-old Lewis rats were used in the present study. Rats were anesthetized by intraperitoneal injection of pentobarbital (30 mg/kg) and were given an injection of either 0.2 ml of antigen–adjuvant emulsion or saline mixed with CFA into the footpad. One week after myosin injection, an osmotic pump (Alzet, Cupertino, CA, USA) was filled with either AM (0.05 μg/kg/min) or PBS for 2 weeks, and implanted subcutaneously between the scapulae. This protocol resulted in the creation of 3 groups ($n=11$ in each group): sham rats given PBS (sham group), myosin-treated rats given PBS (control group), and myosin-treated rats given AM (AM group). The dose of AM used in this study has anti-apoptotic effects without significant hypotension [8]. The investigation conforms with the Guide for the Care and Use of Laboratory Animals published by the US National Institutes of Health.

2.2. Histopathology

After completion of hemodynamic measurements on day 21 post-myosin injection, the heart was excised above the origin of the great vessels, and ventricular weight was recorded. Midventricular portions of the heart were formalin-fixed and embedded in paraffin, and 4 μm-sections were cut and stained with hematoxylin and eosin (H&E). H&E-stained sections were graded by a cardiovascular pathologist (H.I-U.) as described previously [17]. Briefly, coagulation necrosis, granulation, inflammation and edema were evaluated without knowledge of the experimental groups on the following scale: 0, no or questionable presence; 1, limited focal distribution less than 25% area of the section; 2, intermediate severity covering less than 50% area of the section; 3, intermediate severity covering greater than 50% and less than 75% area of the section; and 4, coalescent and extensive foci more than 75% area to the entirety of the transversely sectioned ventricular tissue (5 fields per rat, $n=8$ in each group).

2.3. Picrosirius red staining

Paraffin-embedded sections were submitted for picrosirius staining for total collagen distribution. Slides were hydrated, placed in Weigert's iron hematoxylin and in Bouin's fluid (70% saturated aqueous picric acid, 5% acetic acid, 25% formalin) for 10 min. The slides were rinsed in distilled water and placed in 0.025% picrosirius red solution overnight. The sections were rinsed, dehydrated, cleared, and mounted. Amount of collagen stain was quantitated using image analysis software on high-powered (×200) cross-sectional images (10 fields per rat, $n=5$ in each group).

2.4. Immunohistochemistry

Paraffin-embedded heart sections were washed in increasing concentrations of ethanol and then in PBS. Immunohistochemical staining of the sections was performed with antibodies raised against macrophage chemoattractant protein-1 (MCP-1) (BD Bioscience Pharmingen, San Jose, CA, USA) or CD68 (DakoCytomation, Glostrup, Denmark), a marker of monocytes and macrophages. The number of CD68-positive cells was counted with a light microscope (×200, 10 fields per rat, $n=6$ in each group). To detect capillary endothelial cells, immunohistochemical staining of the sections was performed with a rabbit polyclonal antibody raised against von Willebrand factor (vWF, DakoCytomation). The number of capillary vessels was counted using a light microscope (×200, 10 fields per rat, $n=6$ in each group).

2.5. Western blot analysis

Western blot was performed as previously described [18]. Briefly, LV tissues were homogenized in 0.1% Tween-20 with a protease inhibitor, loaded (40 μg) on a 7.5% sodium dodecyl sulfate-polyacrylamide gel, and blotted onto a polyvinylidene fluoride membrane (Millipore, Billerica, MA, USA). After blocking for 2 h, membranes were incubated with MMP-2 (Laboratory Vision, Fremont, CA, USA) or MMP-9

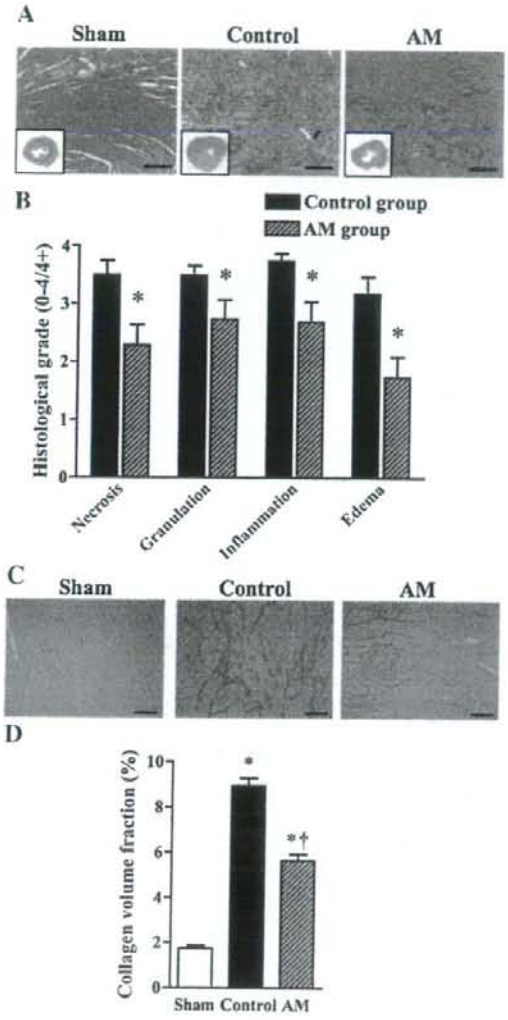

Fig. 1. Pathological findings in acute myocarditis after AM infusion. A: Representative H&E staining of myocardial sections showed markedly decreased inflammation and tissue necrosis in AM-treated hearts as compared to control hearts. Insets are transverse sections of myocardial freewall. B: Semi-quantitative histological grades for necrosis and tissue granulation as well as for inflammation and edema were significantly lower in AM-treated hearts as compared to control hearts ($n=8$ in each group). Sham tissues exhibited no measurable pathological changes. Data are mean±S.E. *, $P<0.05$ vs. control. C: Representative picrosirius staining showed decreased collagen deposition in AM-treated hearts as compared to control hearts. D: Collagen volume fraction in 10 random representative fields (×200) confirmed a significant decrease in AM-treated hearts *vs.* control hearts ($n=5$ in each group). Scale bars: 50 μm. Data are mean±S.E. *, $P<0.05$ vs. sham; †, $P<0.05$ *vs.* control.

(Chemicon, Temecula, CA, USA) rabbit polyclonal antibodies (1:200), then incubated with peroxidase labeled with secondary antibody (1:1000). Positive protein bands were visualized with an ECL kit (GE Healthcare, Piscataway, NJ, USA) and measured by densitometry. A mouse polyclonal antibody against β-actin (Santa Cruz Biotechnology, Santa Cruz, CA, USA) was used as a control ($n=5$ in each group).

2.6. Quantitative real-time reverse transcription-polymerase chain reaction (RT-PCR)

Heart tissues ($n=5$ in each group) were homogenized with TissueLyser (Qiagen, Hilden, Germany). Total RNA was extracted using RNeasy Mini Kit (Qiagen), followed by reverse transcription into cDNA using the avian myeloblastosis virus transcriptase (Ambion, Austin, TX, USA), according to the manufacturers' protocol. PCR amplification was performed in 50 μl containing 1 μl of cDNA and 25 μl of Power SYBR Green PCR Master Mix (Applied Biosystems, Foster City, CA, USA). The following sequence-specific primers were used for TGF-β, as described previously [19]: forward, 5′-GTTCTTCAATACGTCAGACATTCG-3′; reverse, 5′-CATTATCTTTGCTGTCACAAGAGC-3′. Glyceraldehyde 3-phosphate dehydrogenase (GAPDH) mRNA amplified from the same samples was served as an internal control: forward, 5′-GAACATCATCCCTGCATCCA-3′; reverse, 5′-CCAGTGAGCTTCCCGTTCA-3′. After an initial denaturation at 95 °C for 10 min, a 2-step cycle procedure was used (denaturation at 95 °C for 15 s, annealing and extension at 60 °C for 1 min) for 40 cycles in a 7700 sequence detector (Applied Biosystems). The data were analyzed with Sequence Detection Systems software.

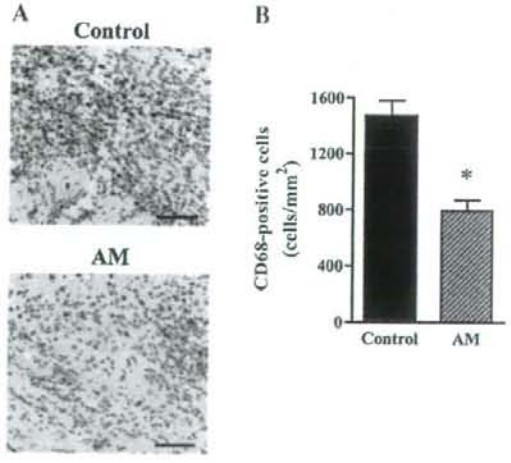

Fig. 2. Infiltration of inflammatory cells in myocardium. A: Immunohistochemical analysis of CD68-positive cell infiltration in myocardium. AM infusion markedly attenuated the increase in CD68-positive cells in myocarditic hearts. Scale bars: 50 μm. B: Semi-quantitative analysis of CD68-positive cell infiltration. CD68-positive cells in 10 random representative high-power fields (×200) confirmed a significant decrease in AM-treated hearts *vs.* control hearts ($n=6$ in each group). Data are mean±S.E. *, $P<0.05$ *vs.* control.

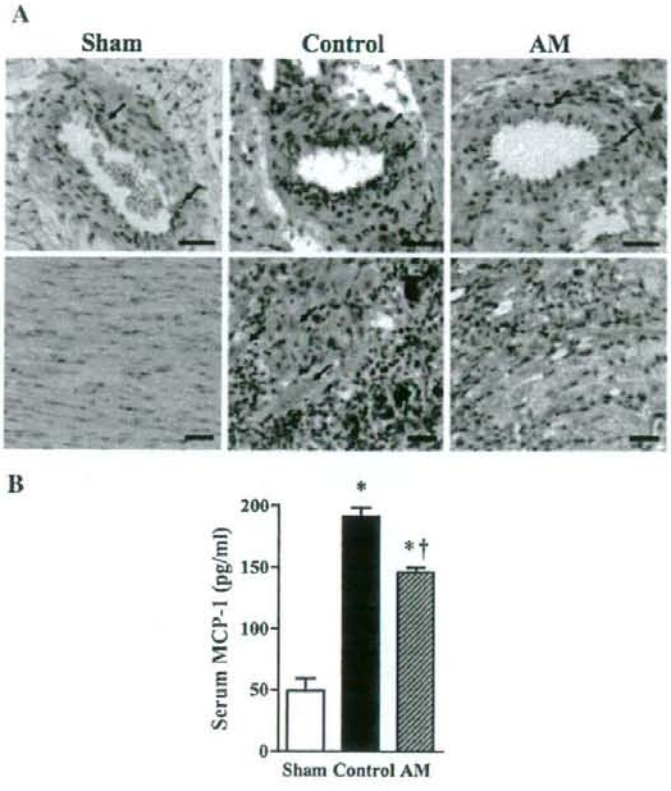

Fig. 3. Effects of AM infusion on MCP-1 expression. A: Representative myocardial sections immunohistochemically stained with anti-MCP-1 antibody showed increased vascular endothelial and myocyte staining of MCP-1 (arrows) and the presence of giant cells (arrowheads) in control hearts as compared to AM-treated hearts. Sham hearts showed subtle endothelial staining. Scale bars: 20 μm. B: Serum MCP-1 level was greatly increased in myocarditic rats. However, the increase in serum MCP-1 was significantly attenuated by AM infusion ($n=6$ in each group). Data are mean±S.E. *, $P<0.05$ *vs.* sham; †, $P<0.05$ *vs.* control.

2.7. Enzyme-linked immunosorbent assay (ELISA)

To investigate the effect of AM infusion on serum MCP-1 level, blood was drawn from the heart before excision ($n=6$ in each group). Blood was centrifuged and serum samples were frozen and stored at −80 °C. Serum MCP-1 level was measured by ELISA according to the manufacturer's instructions (Invitrogen, Carlsbad, CA, USA).

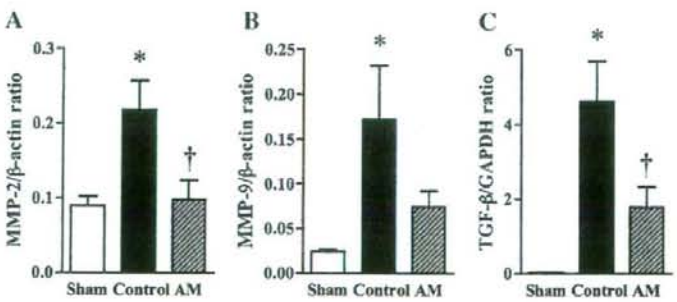

Fig. 4. Effects of AM infusion on MMP and TGF-β expression. A and B: Western blot analysis for MMP-2 (A) and -9 (B) expression. Levels of MMP-2 and -9 were significantly increased in control hearts. MMP-2 expression was markedly decreased by AM infusion, and MMP-9 expression tended to be decreased after AM infusion ($n=5$ in each group). C: Quantitative real-time reverse transcription-polymerase chain reaction (RT-PCR) for TGF-β expression. Expression of TGF-β was increased in myocarditis and significantly decreased by AM treatment ($n=5$ in each group). Data are mean±S.E. *, $P<0.05$ *vs.* sham; †, $P<0.05$ *vs.* control.

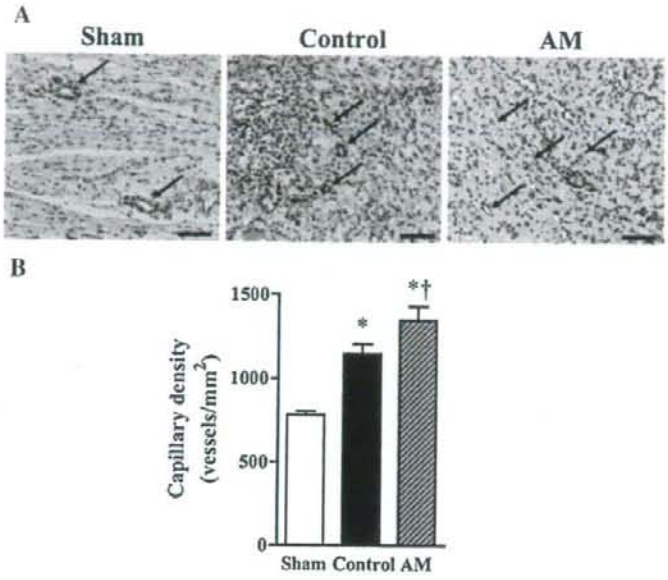

Fig. 5. Increased endothelial regeneration with AM infusion. A: Immunohistochemical demonstration of von Willebrand factor in myocardium. Arrows indicate microvasculature. Scale bars: 20 μm. B: Capillary density measured in 10 random representative high-power fields (×200) showed a significant increase in control hearts and a further increase in AM-treated hearts *vs.* sham hearts (n=6 in each group). Data are mean±S.E. *, P<0.05 *vs.* sham; †, P<0.05 *vs.* control.

2.8. Hemodynamic study

Hemodynamic measurements were taken on day 21 post-myosin injection (n=7 in each group). Rats were anesthetized by intraperitoneal injection of pentobarbital sodium (30 mg/kg) as a supplement to maintain mild anesthesia. A 1.5 Fr micromanometer-tipped catheter (Millar Instruments, Houston, TX, USA) was advanced into the left ventricle through the right carotid artery, and a polyethylene catheter (PE-50) was advanced into the right ventricle through the right jugular vein to measure right ventricular pressure. Heart rate was also monitored by electrocardiography. As hemodynamic indices, heart rate, mean arterial pressure, LV end-diastolic pressure, maximum dP/dt, and minimum dP/dt were used.

2.9. Echocardiography

Echocardiography was performed on day 21 post-myosin injection. A 12-MHz probe was placed in the left 4th intercostal space for M-mode imaging using 2D echocardiography (Sonos 5500, Philips, Bothell, WA, USA). M-mode tracings were obtained at the level of the papillary muscles. Anterior and posterior end-diastolic wall thickness, left ventricular (LV) end-diastolic and end-systolic dimension, LV fractional shortening (FS), and LV ejection fraction (EF) were measured in three consecutive cardiac cycles by the American Society for Echocardiology leading-edge method (n=10 in each group). EF and FS were calculated from the following formula, respectively:

$$EF = (\text{end-diastolic volume} - \text{end-systolic volume}) / \text{end-diastolic volume}$$

$$FS = (\text{end-diastolic diameter} - \text{end-systolic diameter}) / \text{end-diastolic diameter}$$

2.10. Statistical analysis

All data were expressed as mean±S.E. Comparisons of parameters among the groups were made by one-way

Table 1
Physiological profiles of three experimental groups

	Sham	Control	AM
Body weight, g	236±2	197±2*	199±2*
Ventricular weight, g	0.70±0.01	1.28±0.02*	1.15±0.03*†
Lung/body weight	4.9±0.4	4.9±0.5	5.0±0.8
Heart rate, bpm	432±10	373±11	393±6
MAP, mm Hg	103±3	77±5*	93±3†
LVSP, mm Hg	127±3	103±5*	117±3†
LVEDP, mm Hg	4±1	21±5*	14±3

Sham, sham rats given vehicle; Control, myosin-treated rats given vehicle; AM, myosin-treated rats given AM; MAP, mean arterial pressure; LVSP, left ventricular systolic pressure; LVEDP, left ventricular end-diastolic pressure. Data are mean±S.E. *P<0.05 *vs.* sham; †P<0.05 *vs.* control. n=7 in each group.

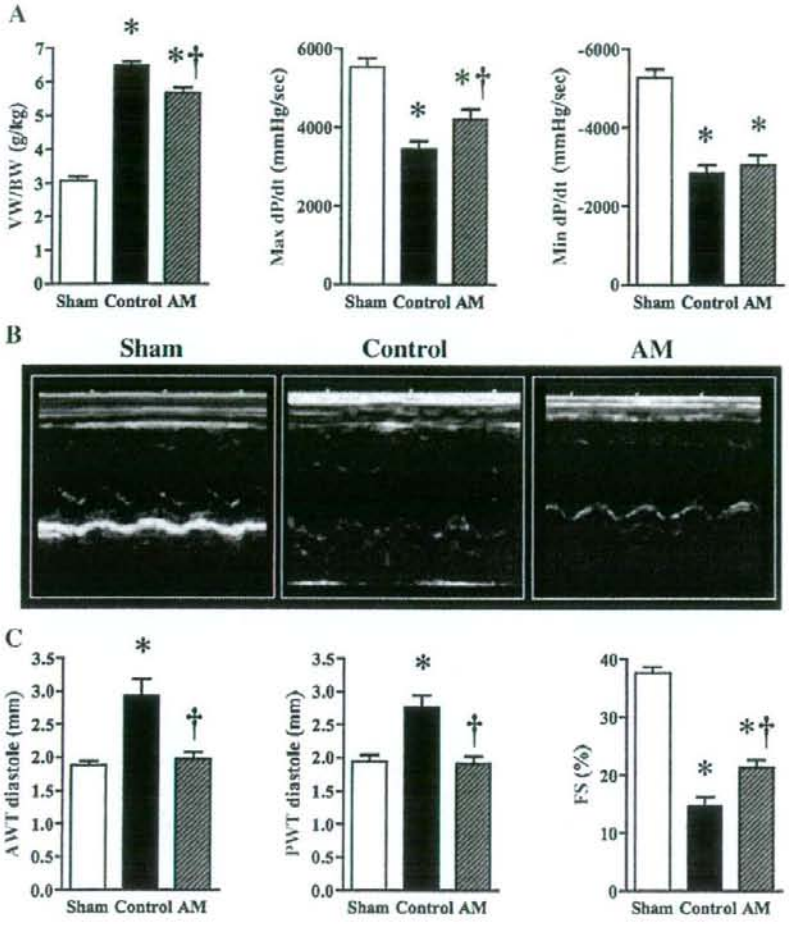

Fig. 6. Effects of AM infusion on physiologic properties and hemodynamic parameters. A: Effects of AM infusion on physiologic properties ($n=7$ in each group). B: Representative echocardiographic images show wall thickening and poor movement in myocarditis and improvement with AM treatment. C: Effects of AM infusion on echocardiographic findings ($n=10$ in each group). VW/BW, ventricular weight/body weight ratio; Max dP/dt, maximum dP/dt; Min dP/dt, minimum dP/dt; AWT, anterior wall thickness; PWT, posterior wall thickness; %FS, %fractional shortening. Data are mean±S.E. *, $P<0.05$ *vs.* sham; †, $P<0.05$ *vs.* control.

ANOVA, followed by Newman–Keuls' test. Comparisons of parameters between two groups were made by Student's *t*-test. A value of $P<0.05$ was considered statistically significant.

3. Results

3.1. Histopathological improvement after AM infusion

Sections of left ventricular tissue demonstrated substantial myocardial necrosis, infiltration of inflammatory cells and edema in the control group, which was significantly limited primarily to areas directly adjacent to arterial vessels with AM treatment (Fig. 1, panel A). Blinded histological grading confirmed decreased myocyte necrosis, granulation, inflammation and tissue edema in the AM group as compared in the control group (Fig. 1, panel B). Picrosirius red staining revealed increased collagen deposition in the control group (Fig. 1, panel C). However, AM infusion attenuated collagen deposition in the myocardium (Fig. 1, panel D).

Table 2
Echocardiographic findings

	Sham	Control	AM
LVDd, mm	4.9±0.1	6.5±0.2*	7.3±0.3*
LVDs, mm	3.1±0.1	5.7±0.2*	5.7±0.3*
EF, %	75±1	35±3*	52±2*†

Sham, sham rats given vehicle; Control, myosin-treated rats given vehicle; AM, myosin-treated rats given AM; LVDd, left ventricular diastolic dimension; LVDs, left ventricular systolic dimension; EF, ejection fraction. Data are mean± S.E. *$P<0.05$ *vs.* sham; †$P<0.05$ *vs.* control. $n=10$ in each group.

3.2. Infiltration of CD68-positive cells in myocardium

A significant decrease in infiltration of CD68-positive inflammatory cells was observed in the AM group as compared to the control group (790±80 *vs.* 1468±109 cells/mm^2; Fig. 2, panel A and B). Sham tissues showed little or no myocardial CD68 positivity (data not shown).

3.3. Expression of MCP-1 after AM infusion

The expression of MCP-1 was increased in myocarditis; it was localized to the vascular endothelium and also in myocytes surrounding and adjacent to the areas of inflammation (Fig. 3, panel A). Heart sections in the AM group showed a partial decrease in MCP-1 expression. Serum MCP-1 level was greatly increased in the control group, whereas a significant decrease was observed in the AM group (Fig. 3, panel B).

3.4. Effects of AM infusion on MMPs and TGF-β expression

Western blotting analysis revealed that myocardial levels of MMP-2 and -9 were significantly increased in the control group. MMP-2 expression was markedly decreased by AM infusion, and MMP-9 expression tended to be decreased after AM infusion (Fig. 4, panel A). Quantitative real-time RT-PCR analysis demonstrated increased expression of TGF-β in the heart of the control group which was significantly attenuated by AM treatment (Fig. 4, panel B). AM infusion did not significantly influence cardiac expression of IL-1β and TNF-α (data not shown).

3.5. Angiogenesis induced by AM infusion

To determine the effect of AM treatment on angiogenesis, vWF-stained heart sections were subjected to capillary density counting. Capillary density was increased in the control group, particularly in areas directly adjacent to tissue necrosis (1146±57 *vs.* 782±21 cells/mm^2, Fig. 5, panel A and B). However, in AM-treated tissues, capillary density was further significantly increased not only in the peri-necrotic areas but also in apparently healthy myocardium (1347±82 *vs.* 1146±57cells/mm^2), suggesting that stimulation of angiogenesis was further augmented by AM treatment.

3.6. Heart weight and hemodynamics after AM infusion

The physiological and catheter-derived functional properties on day 21 post-myosin injection are summarized in Table 1 and Fig. 6, panel A. Myocarditic hearts showed significantly increased heart weight to body weight ratio, which was decreased by AM treatment. AM treatment also significantly improved maximum dP/dt. For both minimum dP/dt and LVEDP, we did not find significant differences. On echocardiography, AM administration significantly attenuated increased wall thickness after acute myocarditis. AM significantly improved LV fractional shortening and ejection fraction, although LVDd did not significantly differ between control and AM groups (Table 2 and Fig. 6, panel B and C).

4. Discussion

In the present study, AM treatment showed the following effects in acute myocarditis: 1) reduced necrosis, inflammation and edema in the myocardium; 2) attenuated expression of MCP-1, MMP-2 and TGF-β; 3) increased capillary density suggestive of angiogenesis; and 4) improved cardiac function.

This experimental autoimmune myocarditis model is triphasic, consisting of an antigen priming phase from days 0 to 14, an autoimmune response phase from days 14 to 21, and a reparative phase thereafter, associated chronically with a dilated cardiomyopathy phenotype [20]. MCP-1 expression is increased in the heart from days 15 to 27 post-myosin injection, and serum MCP-1 level is elevated from days 15 to 24 [21]. We treated rats with AM at 1 week after myosin injection, corresponding to an early time point in the disease process. Pathological examination demonstrated that infusion of AM attenuated myocyte necrosis and inflammation in acute myocarditis. This observation was supported by a decrease in infiltration of CD68-positive inflammatory cells in the myocardium. Interestingly, both MCP-1 expressions in the myocardium and serum MCP-1 level were decreased after AM infusion. MCP-1 is a member of the C–C subfamily of chemokines with chemoattractant activity for major inflammatory cells such as monocytes and T lymphocytes [22], and this model of acute myocarditis has previously been shown to be associated with MCP-1 [21]. Thus, the decrease in CD68-positive cell infiltration in the myocardium following this treatment may be attributable to inhibition of MCP-1 production by AM. The inhibitory effect of AM on MCP-1 expression is consistent with a previous *in vitro* study showing that AM inhibited pressure-induced MCP-1 expression in mesangial cells [23]. Recently, it has been demonstrated that AM has anti-inflammatory effects through modulation of macrophage migration inhibitory factor secretion [24]. Importantly, overexpression of MCP-1 induces myocarditis and subsequent development of heart failure [25]. These findings suggest that the inhibitory effect on MCP-1 expression and subsequent anti-inflammatory effect of AM are possible mechanisms of the improvement in acute myocarditis.

We found a significant increase in heart weight to body weight ratio and wall thickness 3 weeks after myosin injection. These results indicate exaggerated edematous changes in myocarditic hearts. Infusion of AM reduced overall heart weight to body weight ratio and wall thickness in myocarditic hearts and attenuated histological edematous changes. Earlier studies have demonstrated that AM decreases vascular congestion and endothelial hyperpermeability in the heart [11], reduces hyperpermeability of cultured endothelial cells and inhibits pulmonary edema [26]. Thus, it is interesting to speculate that the attenuation of edematous changes in the

heart may be attributable to reduction of endothelial hyperpermeability by AM.

In the present study, AM infusion significantly increased the capillary density in myocarditic hearts. In fact, earlier studies have demonstrated angiogenic properties of AM *in vitro* and *in vivo* [27–29]. Importantly, improvement in myocardial vascular supply has been shown to decrease necrosis and inflammation in viral myocarditis [30,31]. These results suggest that AM-induced angiogenesis in the myocardium may be responsible for the improvement in acute myocarditis, which was indicated by reduced necrosis and inflammation in myocarditic hearts.

As previously mentioned, experimental autoimmune myocarditis chronically develops into a dilated cardiomyopathy phenotype [20]. MMPs have been associated with left ventricular remodeling [32] and here we showed increased expression of MMP-2 and -9 as well as increased collagen deposition in myocarditic hearts. In the present study, AM treatment significantly reduced both MMP-2 expression and collagen deposition. In addition, our observation demonstrated that the expression of TGF-β, a profibrogenic factor, was also attenuated by AM treatment. It has been demonstrated that AM decreases the expression of TGF-β in experimental mesangioproliferative glomerulonephritis [33]. These results suggest that AM may have beneficial effects on myocardium, possibly through regulation of factors involved in LV remodeling. In the present study, LVDd did not significantly differ between the control and AM groups. However, it should be noted that AM significantly reduced wall thickness possibly due to reduction of myocardial edema, leading to a slight increase in the inner diameter of the LV and a significant increase in ejection fraction. The major effect of AM was to reduce myocardial edema but not remodeling, despite reducing biochemical markers of remodeling.

Earlier studies have shown that short-term infusion of AM decreases arterial pressure and increases cardiac output in patients with acute heart failure [5]. These findings suggest that the improvement in cardiac function after acute myocarditis may be mediated partly by the hemodynamic effects of AM. However, despite the well-characterized vasorelaxant properties of AM [4], there was a significant increase in mean arterial pressure after AM treatment in our model. These findings suggest that AM induced limited direct hemodynamic action. Taking these findings together, the improvement of cardiac function after AM treatment may have been mediated by the improvement of pathological findings including necrosis, inflammation and edema in the myocardium rather than by AM-induced hemodynamic effects.

In conclusion, infusion of AM improved cardiac function and pathological findings including inflammatory infiltration and edema in a rat model of acute myocarditis. The beneficial effects of AM may occur at least in part by inhibitory effects on MCP-1, MMP-2 and TGF-β, and by enhancement of angiogenesis after acute myocarditis. Thus, infusion of AM may be a potent therapeutic strategy for acute myocarditis.

Acknowledgements

This work was supported by research grants for Cardiovascular Disease (16C-6 and 17A-1) and Comprehensive Research on Aging and Health from the Ministry of Health, Labour and Welfare, the Program for Promotion of Fundamental Studies in Health Sciences of the National Institute of Biomedical Innovation (NIBIO); and Health and Labor Sciences Research Grants (Human Genome Tissue Engineering 009).

References

[1] Levi D, Alejos J. Diagnosis and treatment of pediatric viral myocarditis. Curr Opin Cardiol 2001;16:77–83.
[2] Liu Z, Yuan J, Yanagawa B, Qiu D, McManus BM, Yang D. Coxsackievirus-induced myocarditis: new trends in treatment. Expert Rev Anti Infect Ther 2005;3:641–50.
[3] Feldman AM, McNamara D. Myocarditis. N Engl J Med 2000;343: 1388–98.
[4] Kitamura K, Kangawa K, Kawamoto M, Ichiki Y, Nakamura S, Matsuo H, et al. Adrenomedullin: a novel hypotensive peptide isolated from human pheochromocytoma. Biochem Biophys Res Commun 1993;192:553–60.
[5] Nagaya N, Satoh T, Nishikimi T, Uematsu M, Furuichi S, Sakamaki F, et al. Hemodynamic renal and hormonal effects of adrenomedullin infusion in patients with congestive heart failure. Circulation 2000;101:498–503.
[6] Oya H, Nagaya N, Furuichi S, Nishikimi T, Ueno K, Nakanishi N, et al. Comparison of intravenous adrenomedullin with atrial natriuretic peptide in patients with congestive heart failure. Am J Cardiol 2000;86:94–8.
[7] Clementi G, Caruso A, Cutuli VM, Prato A, Mangano NG, Amico-Roxas M. Antiinflammatory activity of adrenomedullin in the acetic acid peritonitis in rats. Life Sci 1999;65:PL203–8.
[8] Okumura H, Nagaya N, Itoh T, Okano I, Hino J, Mori K, et al. Adrenomedullin infusion attenuates myocardial ischemia/reperfusion injury through the phosphatidylinositol 3-kinase/Akt-dependent pathway. Circulation 2004;109:242–8.
[9] Iwase T, Nagaya N, Fujii T, Itoh T, Ishibashi-Ueda H, Yamagishi M, et al. Adrenomedullin enhances angiogenic potency of bone marrow transplantation in a rat model of hindlimb ischemia. Circulation 2005;111: 356–62.
[10] Tsuruda T, Kato J, Kitamura K, Kuwasako K, Imamura T, Koiwaya Y, et al. Adrenomedullin: a possible autocrine or paracrine inhibitor of hypertrophy of cardiomyocytes. Hypertension 1998;31:505–10.
[11] Chu DQ, Smith DM, Brain SD. Studies of the microvascular effects of adrenomedullin and related peptides. Peptides 2001;22:1881–6.
[12] Kodama M, Matsumoto Y, Fujiwara M, Zhang SS, Hanawa H, Itoh E, et al. Characteristics of giant cells and factors related to the formation of giant cells in myocarditis. Circ Res 1991;69:1042–50.
[13] Kodama M, Matsumoto Y, Fujiwara M, Masani F, Izumi T, Shibata A. A novel experimental model of giant cell myocarditis induced in rats by immunization with cardiac myosin fraction. Clin Immunol Immunopathol 1990;57:250–62.
[14] Fairweather D, Kaya Z, Shellam GR, Lawson CM, Rose NR. From infection to autoimmunity. J Autoimmun 2001;16:175–86.
[15] Cunningham MW. T cell mimicry in inflammatory heart disease. Mol Immunol 2004;40:1121–7.
[16] O'Connell JBRD. Myocarditis and specific myocardial diseases. New York: McGraw-Hill; 1994. Pages.
[17] Yanagawa B, Spiller OB, Choy J, Luo H, Cheung P, Zhang HM, et al. Coxsackievirus B3-associated myocardial pathology and viral load reduced by recombinant soluble human decay-accelerating factor in mice. Lab Invest 2003;83:75–85.
[18] Nagaya N, Kangawa K, Itoh T, Iwase T, Murakami S, Miyahara Y, et al. Transplantation of mesenchymal stem cells improves cardiac function in a rat model of dilated cardiomyopathy. Circulation 2005;112:1128–35.

[19] Hanawa H, Abe S, Hayashi M, Yoshida T, Yoshida K, Shiono T, et al. Time course of gene expression in rat experimental autoimmune myocarditis. Clin Sci (Lond) 2002;103:623–32.
[20] Kodama M, Hanawa H, Saeki M, Hosono H, Inomata T, Suzuki K, et al. Rat dilated cardiomyopathy after autoimmune giant cell myocarditis. Circ Res 1994;75:278–84.
[21] Fuse K, Kodama M, Hanawa H, Okura Y, Ito M, Shiono T, et al. Enhanced expression and production of monocyte chemoattractant protein-1 in myocarditis. Clin Exp Immunol 2001;124:346–52.
[22] Rollins BJ. Chemokines. Blood 1997;90:909–28.
[23] Iwamoto M, Osajima A, Tamura M, Suda T, Ota T, Kanegae K, et al. Adrenomedullin inhibits pressure-induced mesangial MCP-1 expression through activation of protein kinase A. J Nephrol 2003;16:673–81.
[24] Wong LY, Cheung BM, Li YY, Tang F. Adrenomedullin is both proinflammatory and antiinflammatory: its effects on gene expression and secretion of cytokines and macrophage migration inhibitory factor in NR8383 macrophage cell line. Endocrinology 2005;146:1321–7.
[25] Kolattukudy PE, Quach T, Bergese S, Breckenridge S, Hensley J, Altschuld R, et al. Myocarditis induced by targeted expression of the MCP-1 gene in murine cardiac muscle. Am J Pathol 1998;152:101–11.
[26] Hippenstiel S, Witzenrath M, Schmeck B, Hocke A, Krisp M, Krull M, et al. Adrenomedullin reduces endothelial hyperpermeability. Circ Res 2002;91:618–25.
[27] Kim W, Moon SO, Sung MJ, Kim SH, Lee S, Kim HJ, et al. Protective effect of adrenomedullin in mannitol-induced apoptosis. Apoptosis 2002;7:527–36.
[28] Tokunaga N, Nagaya N, Shirai M, Tanaka E, Ishibashi-Ueda H, Harada-Shiba M, et al. Adrenomedullin gene transfer induces therapeutic angiogenesis in a rabbit model of chronic hind limb ischemia: benefits of a novel nonviral vector gelatin. Circulation 2004;109:526–31.
[29] Nagaya N, Mori H, Murakami S, Kangawa K, Kitamura S. Adrenomedullin: angiogenesis and gene therapy. Am J Physiol Regul Integr Comp Physiol 2005;288:R1432–7.
[30] Lee JK, Zaidi SH, Liu P, Dawood F, Cheah AY, Wen WH, et al. A serine elastase inhibitor reduces inflammation and fibrosis and preserves cardiac function after experimentally-induced murine myocarditis. Nat Med 1998;4:1383–91.
[31] Ono K, Matsumori A, Shioi T, Furukawa Y, Sasayama S. Contribution of endothelin-1 to myocardial injury in a murine model of myocarditis: acute effects of bosentan an endothelin receptor antagonist. Circulation 1999;100:1823–9.
[32] Tsuruda T, Costello-Boerrigter LC, Burnett JC. Matrix metalloproteinases: pathways of induction by bioactive molecules. Heart Fail Rev 2004;9:53–61.
[33] Plank C, Hartner A, Klanke B, Geissler B, Porst M, Amann K, et al. Adrenomedullin reduces mesangial cell number and glomerular inflammation in experimental mesangioproliferative glomerulonephritis. Kidney Int 2005;68:1086–95.

nature medicine

Monolayered mesenchymal stem cells repair scarred myocardium after myocardial infarction

Yoshinori Miyahara[1,9], Noritoshi Nagaya[1,9], Masaharu Kataoka[1], Bobby Yanagawa[1], Koichi Tanaka[1], Hiroyuki Hao[2], Kozo Ishino[3], Hideyuki Ishida[4], Tatsuya Shimizu[5], Kenji Kangawa[6], Shunji Sano[3], Teruo Okano[5], Soichiro Kitamura[7] & Hidezo Mori[8]

© 2006 Nature Publishing Group http://www.nature.com/naturemedicine

Mesenchymal stem cells are multipotent cells that can differentiate into cardiomyocytes and vascular endothelial cells. Here we show, using cell sheet technology, that monolayered mesenchymal stem cells have multipotent and self-propagating properties after transplantation into infarcted rat hearts. We cultured adipose tissue–derived mesenchymal stem cells characterized by flow cytometry using temperature-responsive culture dishes. Four weeks after coronary ligation, we transplanted the monolayered mesenchymal stem cells onto the scarred myocardium. After transplantation, the engrafted sheet gradually grew to form a thick stratum that included newly formed vessels, undifferentiated cells and few cardiomyocytes. The mesenchymal stem cell sheet also acted through paracrine pathways to trigger angiogenesis. Unlike a fibroblast cell sheet, the monolayered mesenchymal stem cells reversed wall thinning in the scar area and improved cardiac function in rats with myocardial infarction. Thus, transplantation of monolayered mesenchymal stem cells may be a new therapeutic strategy for cardiac tissue regeneration.

Myocardial infarction, a main cause of heart failure, leads to loss of cardiac tissue and impairment of left ventricular function. Therefore, restoring the scarred myocardium is desirable for the treatment of heart failure. Although needle injections of bone marrow cells into the myocardium have been performed for cardiac regeneration[1–5], it is difficult to reconstruct sufficient cardiac mass in the thinned scar area after myocardial infarction.

Recently, our colleagues have developed cell sheets using temperature-responsive culture dishes[6]. These cell sheets allow for cell-to-cell connections and maintain the presence of adhesion proteins because enzymatic digestion is not needed[7–10]. Therefore, cell sheet transplantation may be a promising strategy for partial cardiac tissue reconstruction. Skeletal myoblasts, fetal cardiomyocytes and embryonic stem cells have been considered as candidates for an implantable cell source[11–13]. It is difficult, however, to produce a multilayered construct requiring a vascular network. Thus, autologous somatic stem cells with self-propagating properties that can induce angiogenesis are a desirable cell source for a transplantable sheet.

Mesenchymal stem cells (MSCs) are multipotent adult stem cells that reside within the bone marrow microenvironment[14,15]. MSCs can differentiate not only into osteoblasts, chondrocytes, neurons and skeletal muscle cells, but also into vascular endothelial cells[16] and cardiomyocytes[17–20]. In contrast to their hematopoietic counterparts, MSCs are adherent and can expand in culture. Recently, MSCs have been isolated from adipose tissue[21–24], which is typically abundant in individuals with cardiovascular disease. Here, we investigated the therapeutic potency of monolayered MSCs derived from adipose tissue using cell sheet technology.

RESULTS

Characteristics of adipose tissue–derived MSCs

We isolated MSCs from subcutaneous adipose tissue of male Sprague-Dawley rats on the basis of the adherent properties of these cells. We obtained $1.7 \times 10^5 \pm 0.2 \times 10^5$ cells from 1 g adipose tissue in a 12-h culture. By day 4 of culture of the minced adipose tissue, spindle-shaped adherent cells were apparent and formed symmetric colonies. After approximately three to four passages, most adherent cells expressed CD29 and CD90 (**Supplementary Fig. 1** online). In contrast, the majority of adherent cells were negative for CD34 and CD45. They were also negative for CD31, a marker for vascular endothelial cells, and negative for α smooth muscle actin (αSMA), a marker for smooth muscle cells. A small fraction of adherent cells expressed CD71, CD106 and CD117. These results were similar to those from bone marrow–derived MSCs[15,22,25] (**Supplementary Fig. 1** online). Using previously described methods[16,22,26], we confirmed that these adipose-derived adherent cells, like bone marrow–derived MSCs, were multipotent, as judged by their ability to differentiate into adipocytes, osteoblasts and vascular endothelial cells. Thus, we

[1]Department of Regenerative Medicine and Tissue Engineering, National Cardiovascular Center Research Institute and [2]Department of Pathology, National Cardiovascular Center, 5-7-1 Fujishirodai, Suita, Osaka, 565-8565, Japan. [3]Department of Cardiovascular Surgery, Okayama University Graduate School of Medicine, Dentistry and Pharmaceutical Sciences, 2-5-1 Shikata-cho, Okayama, 700-8555, Japan. [4]Department of Physiology, School of Medicine, Tokai University, Bohseidai, Isehara, Kanagawa, 259-1193, Japan. [5]Institute of Advanced Biomedical Engineering and Science, Tokyo Woman's Medical University, 8-1 Kawada-cho, Shinjuku-ku, Tokyo, 162-8666, Japan. [6]Department of Biochemistry, National Cardiovascular Center Research Institute and [7]Department of Cardiovascular Surgery, National Cardiovascular Center and [8]Department of Cardiac Physiology, National Cardiovascular Center Research Institute, 5-7-1 Fujishirodai, Suita, Osaka, 565-8565, Japan. [9]These authors contributed equally to this work. Correspondence should be addressed to N.N. (nnagaya@ri.ncvc.go.jp) or H.M. (hidemori@ri.ncvc.go.jp).

Received 9 August 2005; accepted 3 March 2006; published online 2 April 2006; doi:10.1038/nm1391

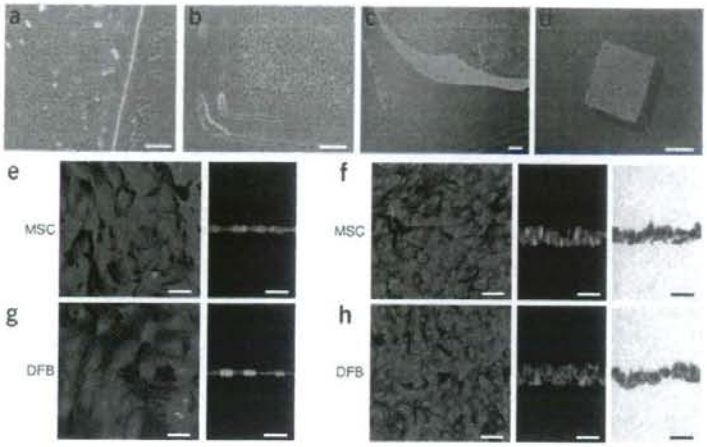

Figure 1 Preparation of monolayered MSCs. (**a**) MSCs 2 d after seeding on a temperature-responsive dish. (**b**) Cultured MSCs expanded to confluence within the square area of the dish by day 3. (**c**) The monolayered MSCs detached easily from the culture dish at 20 °C. (**d**) The completely detached monolayered MSCs were identified as a 12 × 12 mm square sheet. (**e–h**) Cross-sectional analysis of GFP-expressing monolayered MSCs and DFBs before detachment (**e** and **g**, confocal images) and after detachment (**f** and **h**, left and center, confocal images; right, Masson trichrome). The thickness of both monolayers was 3.5-fold greater than the thickness before detachment, and constituent cells were compacted. Scale bars in **a–c**, 100 μm; in **d**, 5 mm; in **e–h**, 20 μm.

© 2006 Nature Publishing Group http://www.nature.com/naturemedicine

confirmed that the majority of adherent cells isolated from adipose tissue were MSCs.

Preparation and transplantation of monolayered MSCs

We cultured adipose tissue–derived MSCs (5×10^5 cells) on temperature-responsive dishes for 3 d until confluent. MSCs were attached on the poly-*N*-isopropylacrylamide (PIPAAm)-grafted area (24 × 24 mm; **Fig. 1a,b**). As the culture temperature was decreased from 37 °C to 20 °C, MSCs detached spontaneously and floated up into the culture medium as a monolayer of MSCs within 40 min (**Fig. 1c,d**). As a control, we prepared dermal fibroblasts (DFBs) by the skin explant technique[27]. DFBs (8×10^5 cells) were cultured on the temperature-responsive dishes, and monolayered DFBs were fabricated as described above. The final cell counts for monolayered MSCs and DFBs before transplantation were $9.4 \pm 0.6 \times 10^5$ and $8.6 \pm 0.6 \times 10^5$ cells, respectively ($n = 6$ each). To identify the thickness of monolayered MSCs, we used green fluorescent protein (GFP)-expressing cell grafts derived from the GFP-transgenic Sprague-Dawley rats. Immediately after detachment, cells became compacted, possibly owing to cytoskeletal tensile reorganization, and the thickness of monolayered MSCs and DFBs was approximately 3.5-fold greater than the thickness before detachment (MSCs, 6.2 ± 0.3 to 21.5 ± 0.8 μm; DFBs, 6.5 ± 0.4 to 22.4 ± 1.1 μm; **Fig. 1e–h**). MSCs on the temperature-responsive dishes were positive for vimentin and slightly positive for collagen type 1, whereas DFBs were positive for both markers (**Fig. 2a**). We transferred detached monolayered MSCs above the myocardial scar (**Fig. 2b**) and then attached them to the surface of the anterior scar (**Fig. 2c**).

Secretion of angiogenic factors from monolayered MSCs

We measured secretion of angiogenic factors from MSCs 24 h after monolayers had formed, equivalent to day 4 after initial cell seeding. The monolayered MSCs secreted significantly larger amounts of angiogenic and antiapoptotic factors such as vascular endothelial growth factor (VEGF) and hepatocyte growth factor (HGF) than did the monolayered DFBs ($P < 0.01$; **Fig. 2d**). The control medium supplemented with 10% fetal calf serum contained less than 5 pg/ml of VEGF or HGF. These results suggest that the paracrine effects of monolayered MSCs on host myocardium are greater than those of monolayered DFBs.

Engraftment and growth of monolayered MSCs

To identify the transplanted cells in myocardial sections, we used GFP-expressing cell grafts derived from the GFP-transgenic Sprague-Dawley rats. We grafted monolayered MSCs or DFBs onto the scar area of the anterior wall (**Fig. 3**). Fluorescence microscopy showed that GFP-expressing monolayered MSCs gradually grew *in situ* and developed into a thick stratum, up to ~600 μm thick over the native tissue at 4 weeks (**Fig. 3a–f**). The engrafted MSC tissue tapered off toward the healthy myocardium (**Fig. 3d,e**), although most of the monolayered MSCs were attached only to the scar area in the anterior wall because of the large infarct. We rarely detected TUNEL-positive MSCs in the sheet (< 1%) 48 h after transplantation (**Fig. 3g**), implying that cell viability in the sheet was maintained. In contrast, we frequently detected TUNEL-positive cells (15% ± 2%) in the DFB sheet, which was observed as a thin layer above the scar. Subsequently, the DFB sheet was undetectable 1 week later. Masson trichrome staining showed increased thickness of the anterior wall and attenuation of left ventricle enlargement after transplantation of monolayered MSCs (**Fig. 3h**), although the infarct size did not differ significantly among the untreated, DFB and MSC groups (**Supplementary Table 1** online).

Reconstruction of cardiac mass

After growth *in situ*, GFP-expressing MSC tissue contained a number of mature vascular structures that had positive staining for von Willebrand factor (vWF) and αSMA (**Fig. 4a,b**). A small fraction of the MSC tissue had positive staining for cardiac troponin T and desmin (**Fig. 4c,d**). On the other hand, a large proportion of the MSC tissue was positive for vimentin, a marker for mesenchymal lineage cells (**Fig. 4e**). The percentages of graft-derived cells that expressed endothelial (vWF), smooth muscle (αSMA), cardiac (troponin T) and mesenchymal (vimentin) markers were 12.2% ± 0.6%, 5.0% ± 0.3%, 5.3% ± 0.3% and 57.8% ± 2.2%, respectively. Notably, based on expression of these markers, two-thirds of vascular endothelial cells, four-fifths of smooth muscle cells and one-twentieth of cardiomyocytes within the MSC tissue were GFP^- and hence were derived from the host. The MSC tissue stained modestly for collagen type 1 (**Fig. 4f**). Picrosirius red staining showed that collagen deposition was found mainly in the extracellular matrix and the epicardial margin of the MSC tissue (**Fig. 4g**). Excluding staining in blood vessels, the MSC tissue was also negative for αSMA, a marker for myofibroblasts (**Fig. 4b**). This phenotype was consistent with properties of MSCs

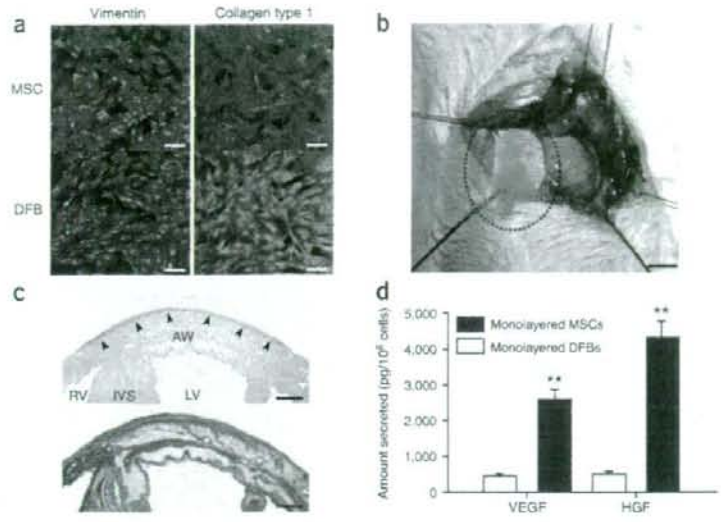

Figure 2 Characteristics of monolayered MSCs. (**a**) Properties of constituent cells in the monolayered grafts. Compared with DFBs (green), MSCs (green) are positive for vimentin (red) and slightly positive for collagen type 1 (red). (**b**) Monolayered MSCs (in the dotted circle) transferred to the infarcted heart. (**c**) Extent of monolayered MSCs 48 h after transplantation (arrows). AW, anterior wall; LV, left ventricle; RV right ventricle; IVS, interventricular septum. (**d**) Comparison of secretion of growth factors between monolayered MSCs and DFBs. $^{**}P < 0.01$ versus DFBs. Scale bar in **a**, 20 μm; in **b**, 5 mm; in **c**, 100 μm.

© 2006 Nature Publishing Group http://www.nature.com/naturemedicine

before transplantation (**Fig. 2a** and **Supplementary Fig. 1** online), suggesting that the MSC tissue includes a number of undifferentiated MSCs. Taken together, the grown MSC tissue was composed of newly formed blood vessels, undifferentiated MSCs and few cardiomyocytes.

Fluorescence *in situ* hybridization analysis

We performed fluorescence *in situ* hybridization (FISH) to detect X and Y chromosomes after sex-mismatched transplantation of monolayered MSCs. We transplanted GFP-expressing monolayered MSCs derived from male rats to female Sprague-Dawley rats that had suffered an infarct. Four weeks later, newly formed cardiomyocytes that were positive for GFP had only one set of X and Y chromosomes, whereas we detected two X chromosomes exclusively in GFP^- host-derived cells (**Fig. 4h**). We counted the X and Y chromosomes in male and female control rats and in the MSC sheet–transplanted rats (**Supplementary Table 2** online), and we did not detect extra copies of the X or Y chromosome in graft-derived GFP^+ cardiomyocytes. When we compared the frequencies of the occurrence of zero, one, two and more than two X chromosomes in the GFP^+ cardiomyocytes with the frequencies in male control cardiomyocytes, the GFP^+ cardiomyocytes did not show an increased proportion of X chromosomes ($0.25 > P > 0.10$, χ^2 test).

Effects of monolayered MSCs on cardiac function

Heart failure developed 8 weeks after coronary ligation, as indicated by an increase in left ventricle end-diastolic pressure (LVEDP) and attenuation of maximum and minimum rate of change in left ventricular pressure (dP/dt). Autologous transplantation of monolayered MSCs, however, resulted in decreased LVEDP (**Fig. 5a**). Left ventricle maximum and minimum dP/dt were significantly improved in the MSC group (**Fig. 5b,c**). We did not observe these hemodynamic improvements in the DFB group. The MSC group also had significantly lower right ventricular weight and lung weight than the DFB and untreated groups 4 weeks after transplantation (**Supplementary Table 1** online). These results suggest that transplantation of monolayered MSCs has beneficial hemodynamic effects in rats with chronic heart failure.

Echocardiographic analysis showed that transplantation of monolayered MSCs significantly increased diastolic thickness of the infarcted anterior wall (**Fig. 5d**). Left ventricle end-diastolic dimension at 8 weeks was significantly smaller in the MSC group than in the DFB and untreated groups (**Fig. 5e**). Transplantation of the monolayered MSCs significantly increased left ventricle fractional shortening (**Fig. 5f**). Left ventricle wall stress in diastole was markedly lower in the MSC group than in the DFB and untreated groups (**Supplementary Table 3** online). Plasma atrial natriuretic peptide (ANP) in the DFB and untreated groups was markedly elevated 8 weeks after myocardial infarction (**Fig. 5g**). Transplantation of the monolayered MSCs inhibited the increase in plasma ANP.

Survival analysis

The Kaplan-Meier survival curve showed that 4-week survival after coronary ligation did not differ significantly between the untreated and MSC groups before transplantation (**Fig. 5h**). Notably, however, no rats died after transplantation of monolayered MSCs. Therefore, the survival rate after transplantation was markedly higher in the MSC group than in the untreated group (4-week survival after transplantation was 100% for the MSC group versus 71% for the untreated group, log-rank test, $P < 0.05$).

DISCUSSION

There are several advantages to monolayered MSC transplantation. First, the self-propagating property of MSCs *in situ* leads to the formation of a thick stratum on the surface of the scarred myocardium. Second, the multipotency of MSCs and their ability to supply angiogenic cytokines allows neovascularization in the MSC tissue. Third, the reconstruction of thick myocardial tissue reduces left ventricle wall stress and results in improvement of cardiac function after myocardial infarction. Finally, a substantial part of the transplanted tissue is composed of undifferentiated MSCs, and it is tempting to speculate that such cells may act against future progressive left ventricle remodeling.

Cellular cardiomyoplasty using needle injections is emerging as a treatment option for individuals with chronic heart failure, but it may be limited by failure to regenerate cardiac mass. The cell sheet allows for cell-to-cell connections owing to the lack a need for enzymatic digestion[6–10]. Thus, the cell sheet has attracted considerable interest as a tool for tissue engineering[28]. Here, we used adipose tissue–derived MSCs as a cellular source for the cell sheet, which resulted in successful autologous transplantation in heterogenic rats without immunological

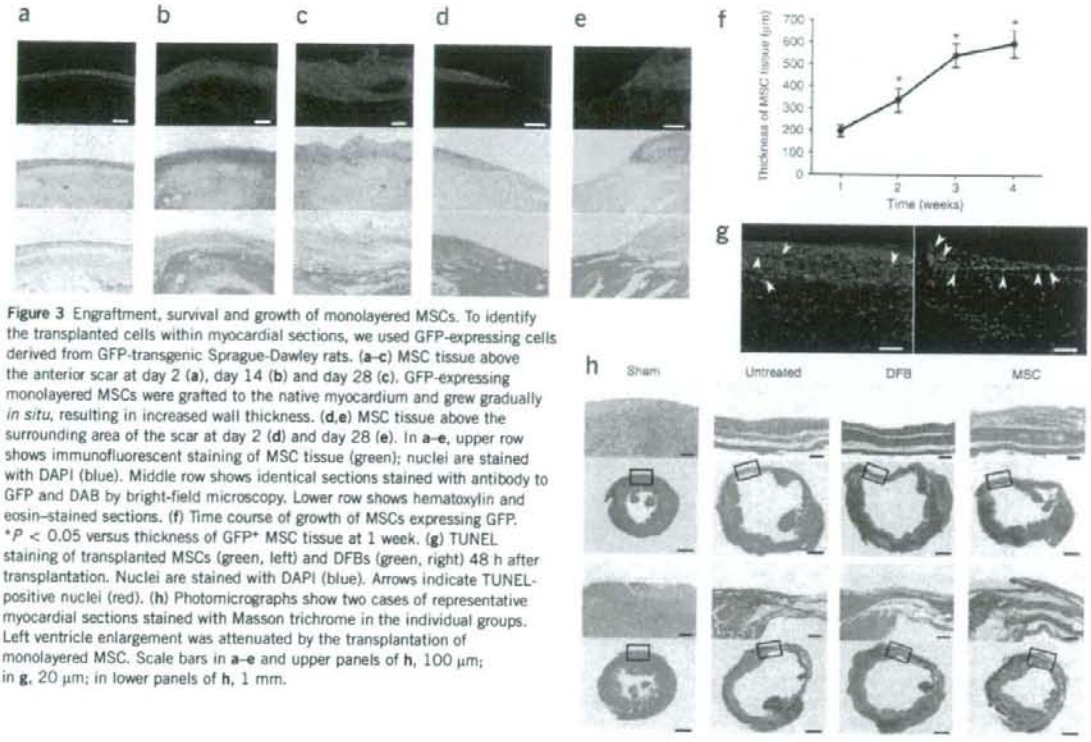

Figure 3 Engraftment, survival and growth of monolayered MSCs. To identify the transplanted cells within myocardial sections, we used GFP-expressing cells derived from GFP-transgenic Sprague-Dawley rats. (**a–c**) MSC tissue above the anterior scar at day 2 (**a**), day 14 (**b**) and day 28 (**c**). GFP-expressing monolayered MSCs were grafted to the native myocardium and grew gradually *in situ*, resulting in increased wall thickness. (**d,e**) MSC tissue above the surrounding area of the scar at day 2 (**d**) and day 28 (**e**). In **a–e**, upper row shows immunofluorescent staining of MSC tissue (green); nuclei are stained with DAPI (blue). Middle row shows identical sections stained with antibody to GFP and DAB by bright-field microscopy. Lower row shows hematoxylin and eosin–stained sections. (**f**) Time course of growth of MSCs expressing GFP. $^*P < 0.05$ versus thickness of GFP$^+$ MSC tissue at 1 week. (**g**) TUNEL staining of transplanted MSCs (green, left) and DFBs (green, right) 48 h after transplantation. Nuclei are stained with DAPI (blue). Arrows indicate TUNEL-positive nuclei (red). (**h**) Photomicrographs show two cases of representative myocardial sections stained with Masson trichrome in the individual groups. Left ventricle enlargement was attenuated by the transplantation of monolayered MSC. Scale bars in **a–e** and upper panels of **h**, 100 μm; in **g**, 20 μm; in lower panels of **h**, 1 mm.

© 2006 Nature Publishing Group http://www.nature.com/naturemedicine

rejection. Using flow cytometry, we did not find any substantial differences between adipose tissue–derived MSCs and bone marrow–derived MSCs, consistent with results from previous studies[22,25]. Adipose-derived MSCs readily attached to and propagated on the temperature-responsive dish. Abdominal subcutaneous adipose tissue is clinically redundant and easily accessible by rapid and minimally invasive surgery such as liposuction. Thus, adipose tissue may serve as a source of stem cells for therapeutic cell sheets.

Here, monolayered MSCs could readily be transferred and grafted to the scarred myocardium without additives or suturing. This may be attributable to cell-to-cell connections as well as extracellular matrix deposits on the basal surface of the monolayered MSCs. Regeneration of myocardial mass is thought to require multilayered constructs of the cell sheet. Unfortunately, however, the lack of a vascular network has limited the formation of a thick construct[10,29]. The transplanted monolayered MSCs thickened gradually, developing into a stratum of up to 600 μm in thickness over the native tissue 4 weeks after transplantation, suggesting that monolayered MSCs have an ability to grow *in situ*. As a result, the transplanted MSC tissue reversed wall thinning of the infarcted myocardium. On the other hand, the fibroblast sheet did not grow *in situ*. It should be noted that the MSC tissue included a large number of newly formed blood vessels. These vessels were composed of graft-derived cells, host-derived cells or both. The MSC sheet secreted a large amount of angiogenic and antiapoptotic cytokines, including VEGF and HGF, as compared with the fibroblast sheet. These results suggest that MSCs induce neovascularization within the sheet not only through their ability to differentiate into vascular cells but also through growth factor–mediated paracrine regulation. Thus, we believe that the angiogenic action of MSCs is important for reconstruction of cardiac mass by the MSC tissue.

Four weeks after transplantation, a small fraction of the engrafted MSCs were positive for cardiac proteins such as cardiac troponin T and desmin, suggesting the presence of cardiomyocytes within the MSC tissue. FISH analysis suggested that the most cardiomyocytes within the MSC tissue were not derived from cell fusion, but we are unable to exclude the possibility that some were. Further studies are necessary to investigate the mechanisms by which MSCs within the MSC tissue regenerate cardiomyocytes. The majority of the MSC tissue was positive for vimentin, a marker for undifferentiated MSCs and fibroblasts. In addition, the majority of MSCs within the graft were negative for collagen type 1 and αSMA, a marker for myofibroblasts. These results suggest that the grown-up MSC tissue is composed of newly formed blood vessels, undifferentiated MSCs and few cardiomyocytes.

We have also shown that transplantation of the monolayered MSCs significantly increased left ventricle maximum dP/dt, decreased LVEDP and inhibited the development of left ventricle enlargement in rats with chronic heart failure secondary to myocardial infarction. These results suggest that transplantation of monolayered MSCs improves cardiac function. But the presence of cardiomyocytes within the MSC tissue seemed to be rare. Thus, this improvement may be explained mainly by growth factor–mediated paracrine effects of the MSC sheet and a decrease in left ventricle wall stress resulting from the thick MSC tissue. Furthermore, no rats treated with the monolayered MSCs died during the study period, although untreated rats died frequently. These results indicate that fatal arrythmogenic problems were not caused by integration of the MSC tissue.